ORGANIC CHEMISTRY FRONTIERS

RESEARCH ARTICLE

View Article Online
View Journal | View Issue

Cite this: *Org. Chem. Front.*, 2022, **9**, 3093

(±)-Spiroganoapplanin A, a complex polycyclic meroterpenoid dimer from *Ganoderma applanatum* displaying potential against Alzheimer's disease†

Xing-Rong Peng,‡[a,b] Rong-Can Luo, ‡[b,c,d] Hai-Guo Su,[a] Lin Zhou,[a] Xiao-Qian Ran,[c,d,b] Ya-Rong Guo,[c,d,e] Yong-Gang Yao *[c,d,b,f] and Ming-Hua Qiu *[a,b]

Received 17th February 2022,
Accepted 18th April 2022

DOI: 10.1039/d2qo00246a

rsc.li/frontiers-organic

(±)-Spiroganoapplanin A (**1**) representing a new subtype of the *Ganoderma* meroterpenoid dimer with a 6/5/5/6/5/6 hexacyclic system was isolated from *Ganoderma applanatum*. Using spectroscopic, X-ray crystallographic and electronic circular dichroism analyses, the structure of the racemic natural product was determined, and its unusual NMR behavior was investigated by variable-temperature NMR experiments. The possible biogenetic pathway for **1** was proposed. Cellular assays showed that (±)-**1**, (+)-**1**, and (−)-**1** all reduce Aβ42 production and inhibit tau phosphorylation through BACE1, CDK5, and GSK3β-mediated pathways, suggesting their potential against Alzheimer's disease.

Introduction

Alzheimer's disease (AD) has seriously affected the lives of middle-aged and elderly individuals. A study has predicted that up to 16 million people could be AD patients by 2050.[1] The histopathological feature of AD mainly consists of brain β-amyloid (Aβ) plaques and neurofibrillary tangles (NFT, composed of hyperphosphorylated tau), which lead to the dysfunction of cognition and eventually to death.[2,3] Current disease models suggest that Aβ triggers tau pathology, with a complex and synergistic interaction between Aβ and tau manifesting at later stages and leading to the progression of AD.[4] The genetic and pathological studies have confirmed that the reduction of Aβ production plays a key role in the treatment of AD.[5,6] Notably, the β-site amyloid precursor protein cleaving enzyme 1 (BACE1) acts as the rate-limiting enzyme,[7,8] and the tau-related phosphatase or kinase, such as glycogen synthase kinase 3β (GSK3β) and cyclin-dependent kinase 5 (CDK5), can modulate tau-phosphorylation.[9,10] Thus, to broaden the research on multi-functional anti-AD drugs, the discovery of novel and promising lead compounds with multiple anti-AD properties is extremely urgent. Therapeutics directed at multiple targets for AD treatment would have more chance of success.[11]

Ganoderma has been widely used as an edible and medicinal mushroom in China for about 2000 years.[12] The ancient Chinese agronomy book *Shennong's Herbal Classic* and *Compendium of Materia Medica* described the medical benefits of *Ganoderma* such as prolonging life-span, keeping health, improving intelligence and memory.[13] Modern pharmacological research studies have also provided evidence of the possible therapeutic effects of *Ganoderma* and its extracts on AD through inhibiting inflammation, resisting oxidation pressure and reducing the aggregation of Aβ.[14–18] Furthermore, *Ganoderma* meroterpenoids (GMs) have been found to possess neuroprotective potential in different *in vitro* models.[19,20] However, the effects of GMs on Aβ production and tau phosphorylation are still unclear.

Inspired by the findings above and our previous studies,[21] we systematically investigated the GMs from the fruiting bodies of *G. applanatum* and isolated (±)-spiroganoapplanin A (**1**) possessing a complex 6/5/5/6/5/6-fused polycyclic skeleton

[a]*State Key Laboratory of Phytochemistry and Plant Resources in West China, Kunming Institute of Botany, Chinese Academy of Science, Kunming 650201, China. E-mail: mhchiu@mail.kib.ac.cn*
[b]*Kunming College of Life Science, University of Chinese Academy of Sciences, Kunming, Yunnan 650204, China*
[c]*Key Laboratory of Animal Models and Human Disease Mechanisms of the Chinese Academy of Sciences & Yunnan Province, Kunming, China*
[d]*KIZ-CUHK Joint Laboratory of Bioresources and Molecular Research in Common Diseases, Kunming Institute of Zoology, Chinese Academy of Sciences, Kunming 650204, China. E-mail: yaoyg@mail.kiz.ac.cn*
[e]*School of Life Sciences, Division of Life Sciences and Medicine, University of Science and Technology of China, Hefei 230026, China*
[f]*CAS Center for Excellence in Brain Science and Intelligence Technology, Chinese Academy of Sciences, Shanghai 200031, China*

†Electronic supplementary information (ESI) available: 1D and 2D NMR, MS spectra, X-ray crystallographic data, and calculated ECD. CCDC 2098350 (**1**). For ESI and crystallographic data in CIF or other electronic format see DOI: **https://doi.org/10.1039/d2qo00246a**

‡These authors contributed equally to this work.

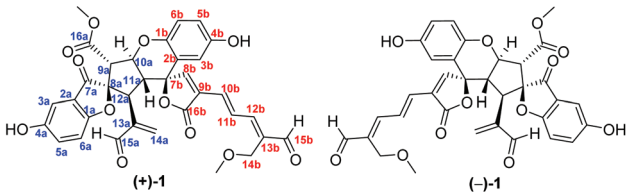

Fig. 1 Structures of (+)-**1** and (–)-**1**.

(Fig. 1). The stereo-structure of **1** was elucidated by a series of 1D and 2D NMR spectra, X-ray diffraction, electronic circular dichroism (ECD) analyses, and variable-temperature NMR experiments. We also proposed a plausible biosynthetic pathway for (±)-**1**. Furthermore, we conducted cellular analyses using human glioma U251 cells stably expressing the human APP mutant (APP-p.K670N/M671L, U251-APP cells) to evaluate the anti-AD activities of the racemic and enantiomeric **1**. The results showed that (±)-**1**, (+)-**1**, and (–)-**1** all showed no apparent toxicity for U251-APP cells, at concentrations of 5 and 20 μM, while significantly decreasing the protein levels of BACE1. Moreover, the enzyme linked immunosorbent assay (ELISA) indicated that they decrease the levels of Aβ42, at a concentration of 20 μM. Western blotting analyses showed that (±)-**1**, (+)-**1**, and (–)-**1** can decrease the protein levels of CDK5, and increase phospho-GSK3β (pGSK3β, Ser9). These results demonstrate that (±)-**1**, (+)-**1**, and (–)-**1** may be potential lead compounds for the development of AD therapeutics.

Results and discussion

The molecular formula of (±)-spiroganoapplanin A (**1**) was determined to be $C_{34}H_{28}O_{12}$ based on positive HRESIMS at *m*/*z* 651.1463 $[M + Na]^+$ (calcd. 651.1473), which indicated 21 degrees of unsaturation. However, the ^{13}C NMR spectrum only showed 28 carbon resonances, which were attributed to two methoxyls, one oxygenated methylene, one sp^3 methine, one oxygenated methine, ten sp^2 methines, one oxygenated quaternary carbon, eight sp^2 quaternary carbons, two aldehyde groups, and two ester carbonyls. Two sets of 1,2,4-trisubstituted phenyl signals {δ_H 6.80 (d, J = 2.7 Hz, H-3a), δ_H 7.14 (dd, J = 8.9 and 2.7 Hz, H-5a), δ_H 6.92 (d, J = 8.9 Hz, H-6a); δ_H 6.30 (d, J = 2.9 Hz, H-3b), δ_H 6.75 (dd, J = 9.0 and 2.9 Hz, H-5b), δ_H 6.84 (d, J = 9.0 Hz, H-6b)} with ABX systems were observed in the ^1H NMR spectroscopic data (298 K) (Table S1†). In addition, one aldehyde proton (δ_H 9.49, s, H-15b), two methoxyl protons (δ_H 3.50, s, H-17a; δ_H 3.32, s, H-17b), one oxygenated methylene proton (δ_H 4.25, d, J = 3.7, H-14b), four sp^2 methine protons (δ_H 8.05, s, H-8b; δ_H 6.83, m, H-10b; δ_H 7.89, dd, J = 15.6 and 11.6 Hz, H-11b; δ_H 7.22, d, J = 11.6 Hz, H-12b) and two methine protons (δ_H 3.82, d, J = 9.7 Hz, H-9a; δ_H 4.85, br s, H-10a) were assigned by 1D NMR and HSQC spectra (298 K). The above information indicated that compound **1** could be a meroterpenoid dimer.

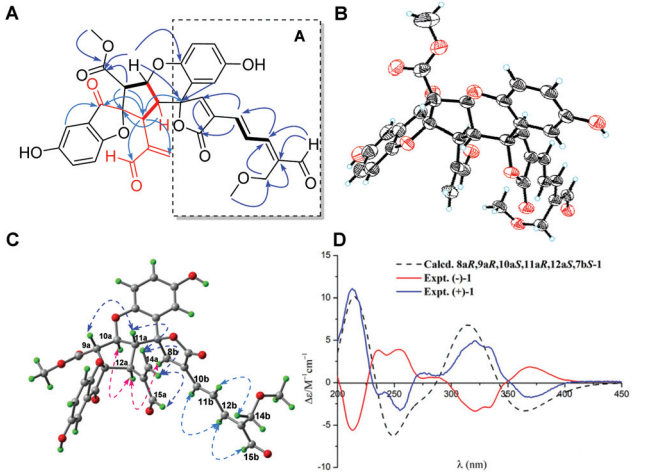

Fig. 2 (A) Selected HMBC correlations (blue arrow, 298 K and light blue arrow, 253 K), ^1H–^1H COSY correlations (bold bond, 298 K and red bold bond, 253 K); (B) ORTEP view of the X-ray structure (±)-**1**; (C) ROESY correlations (double-headed arrow) of **1**; (D) calculated and experimental ECD curves of (±)-**1**.

Furthermore, in the HMBC spectrum (298 K) (Fig. 2A), H-3b showed a correlation with an oxygenated quaternary carbon (δ_C 87.5, C-7b). Meanwhile, an sp^2 methine proton (δ_H 8.05, s, H-8b) correlated with C-7b, C-16b (δ_C 171.7), and C-10b (δ_C 130.7). Moreover, the HMBC correlations of H-10b with C-16b, C-8b, C-11b, and C-12b, of H-11b with C-9b, C-12b, and C-13b, of H-12b with C-13b, C-14b, and C-15b, of the methoxyl (δ_H 3.32, s) with C-14b, along with the ^1H–^1H COSY correlations of H-10b/H-11b/H-12b illustrated the presence of fraction A (Fig. 2A).

Additionally, an oxygenated methine proton (δ_H 4.85, br s, H-10a) showed HMBC correlations with C-1b (δ_C 153.3) and C-16a (δ_C 170.1), the methoxyl (δ_H 3.50, s) correlated with C-16a, while the correlation of H-10a/H-9a was observed in the ^1H–^1H COSY spectrum (298 K), which confirmed the presence of a methyl propionate fraction.

Notably, the lack of useful 1D and 2D NMR signals led to the failure of the further structural elucidation. Fortunately, a crystal was obtained from methanol, and the X-ray crystallographic analysis (Cu Kα) unambiguously confirmed compound **1** to be a meroterpenoid dimer with a 6/5/5/6/5/6 hexacyclic skeleton containing two spiro motifs, as shown in Fig. 2B. Interestingly, given the single crystal structure, it was puzzling that the 1D NMR signals in the red part (Fig. 2A) were hardly observable (Table S1†), which could be caused by the conformational exchange that led to the variation in the magnetic environment of nuclei in varying degrees depending on temperature.[22–24] Further structural analysis suggested that the hindered rotation about the C-12a–C-13a bond might break the conformational averaging and the slow exchange at room temperature caused the line broadening.

To certify this hypothesis, a variable-temperature NMR experiment was carried out. The ^1H and ^{13}C NMR signals in

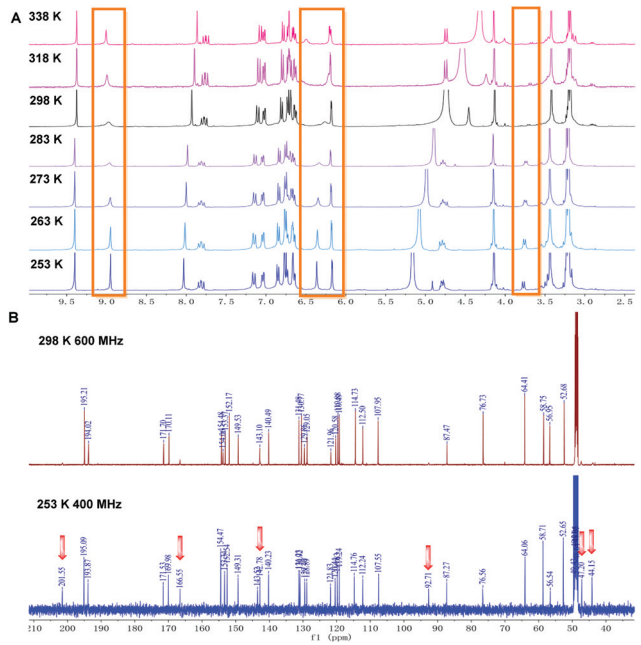

Fig. 3 (A) The comparison of the ^{1}H NMR (400 MHz, CD_3OD) spectra of **1** at various temperatures. (B) The comparison of the ^{13}C NMR spectra of **1** at 298 K (150 MHz, CD_3OD) and 253 K (100 MHz, CD_3OD). Red squares and red arrows represent disappeared signals in the structure of **1**.

the red part (Fig. 2A) appeared as the temperature was lowered (Fig. 3). Careful analysis of the HMBC spectrum (253 K) showed that the correlations of H-3a, H-9a, and H-12a with the ketone carbonyl (δ_C 200.2, C-7a), of H-10a with C-8a (δ_C 91.3), of H-12a with C-14a (δ_C 142.3), C-15a (δ_C 192.5), C-8a (δ_C 91.3), and C-7b (δ_C 86.2), and of H-11a with C-7b. The ^{1}H–^{1}H COSY correlations of H-9a/H-10a/H-11a/H-12a and a series of ROESY correlations of H-9a/H-11a/H_a-14a, of H-10a/H-12a/H-8b, of H-10b/H-12b/H-15b, and of H-11b/H-14b were observed (Fig. 2C). These 2D NMR correlations further confirmed its structure and relative configuration.

The X-ray crystallographic data also proved that **1** was a pair of enantiomers and its relative configuration was determined to be 8a*R*′, 9a*R*′, 10a*S*′, 11a*R*′, 12a*S*′, 7b*S*′. The further chiral separation resulted in the isolation of (+)-**1** and (−)-**1**, showing opposite specific rotation values and CD curves. The calculation of ECD was conducted based on the B3LYP/6-311+G(d,p) theory method and the result exhibited that the experimental CD curve of (+)-**1** was corresponding to that of 8a*R*,9a*R*,10a*S*,11a*R*,12a*S*,7b*S*-**1**. Thus, the absolute configurations of (+)-**1** and (−)-**1** were assigned as 8a*R*,9a*R*,10a*S*,11a*R*,12a*S*,7b*S* and 8a*S*,9a*S*,10a*R*,11a*S*,12a*R*,7b*R*, respectively (Fig. 2D).

Diels–Alder or hetero-Diels–Alder reactions are well known to play key roles in the construction of complex natural products, especially terpenoid dimers.[25] Until now, more than 20 GM dimers have been isolated from *Ganoderma* genus,[26–31] and the majority of them are believed to arise through the dimerization involving the Diels–Alder reaction.[27,31] While the key tetrahydro-2*H*-pyan ring of (±)-spiroganoapplanin A (**1**) is produced by a hetero-Diels–Alder reaction of two molecules of the formicin D-derived intermediate I (Scheme S1†), subsequent oxidation and cyclization also play significant roles in the formation of key intermediates and the novel molecular architecture of **1**.

AD is crucially related to Aβ plaques, which not only induce oxidative stress but also activate the NLRP3 inflammasome, releasing inflammatory cytokine IL-1β to trigger neuroinflammation.[32] In addition, tau phosphorylation can result in NFT, which is an important histopathological feature of AD.[2] Our previous studies showed that GMs had anti-oxidative, anti-inflammatory and neuroprotective activities, suggesting that GMs could exhibit potential anti-AD effects.[27,33,34] Thus, it was of interest to investigate the inhibition of Aβ production and tau phosphorylation by (±)-**1**, (+)-**1**, and (−)-**1** in order to explore their anti-AD' effect.

We conducted cellular analyses using human glioma U251 cells stably expressing the human APP mutant (APP-p. K670N/M671L) (U251-APP cells), a cellular AD model that was created in our previous studies.[35–37] While DMSO (dimethyl sulfoxide) was used as the solvent and the control, gemfibrozil approved by the U.S. Food and Drug Administration primarily for treating hyperlipidemia[38,39] was used as a positive control in cellular assays as it could reduce Aβ production[40] and increase Aβ clearance.[41] At concentrations of 5 μM and 20 μM, (±)-**1**, (+)-**1**, and (−)-**1** show no apparent toxicity for U251-APP cells (Fig. 4A). Using the western blotting analyses, we checked the protein levels of BACE1 (β-secretase), the first protease that processes the amyloid precursor protein (APP) to produce toxic Aβ and therefore plays a key role in the pathogenesis of AD,[42,43] and the components of γ-secretase including PSEN1 (presenilin 1), PSEN2 (presenilin 2), NCSTN (nicastrin) and PEN2 (PSENEN; presenilin enhancer, γ-secretase subunit). (±)-**1**, (+)-**1**, and (−)-**1** significantly decreased the protein level of BACE1 at concentrations of 5 and 20 μM. They decreased the protein levels of NCSTN and PSEN1, but had no significant effect on the protein levels of PSEN2 and PEN2 in U251-APP cells, at a concentration of 20 μM (Fig. 4B–D). Furthermore, we measured the levels of Aβ42 species, which play major synaptotoxic roles in AD.[44] In the culture supernatant of U251-APP cells treated with (±)-**1**, (+)-**1**, and (−)-**1**, they significantly decreased the levels of Aβ42 (20 μM), as determined by the enzyme linked immunosorbent assay (ELISA) (Fig. 4E). Interestingly, the effects of (±)-**1** on Aβ42 accumulation were seemingly better than those of gemfibrozil (50 μM), suggesting its potential to prevent Aβ production and downstream consequence therefrom.

Additionally, we evaluated anti-tau phosphorylation effects of (±)-**1**, (+)-**1**, and (−)-**1**. Dinaciclib, a CDK5 selective inhibitor,[45] was used as a positive treatment in this assay. Western blotting analyses showed that (±)-**1**, (+)-**1**, and (−)-**1** can significantly decrease the protein levels of CDK5, and increase phospho-GSK3β (Ser9) (pGSK3β) at concentrations of 5 μM and 20 μM (Fig. 4F–H), suggesting their potential to inhibit GSK-3β enzymatic activity.[46] Moreover, the levels of phospho-

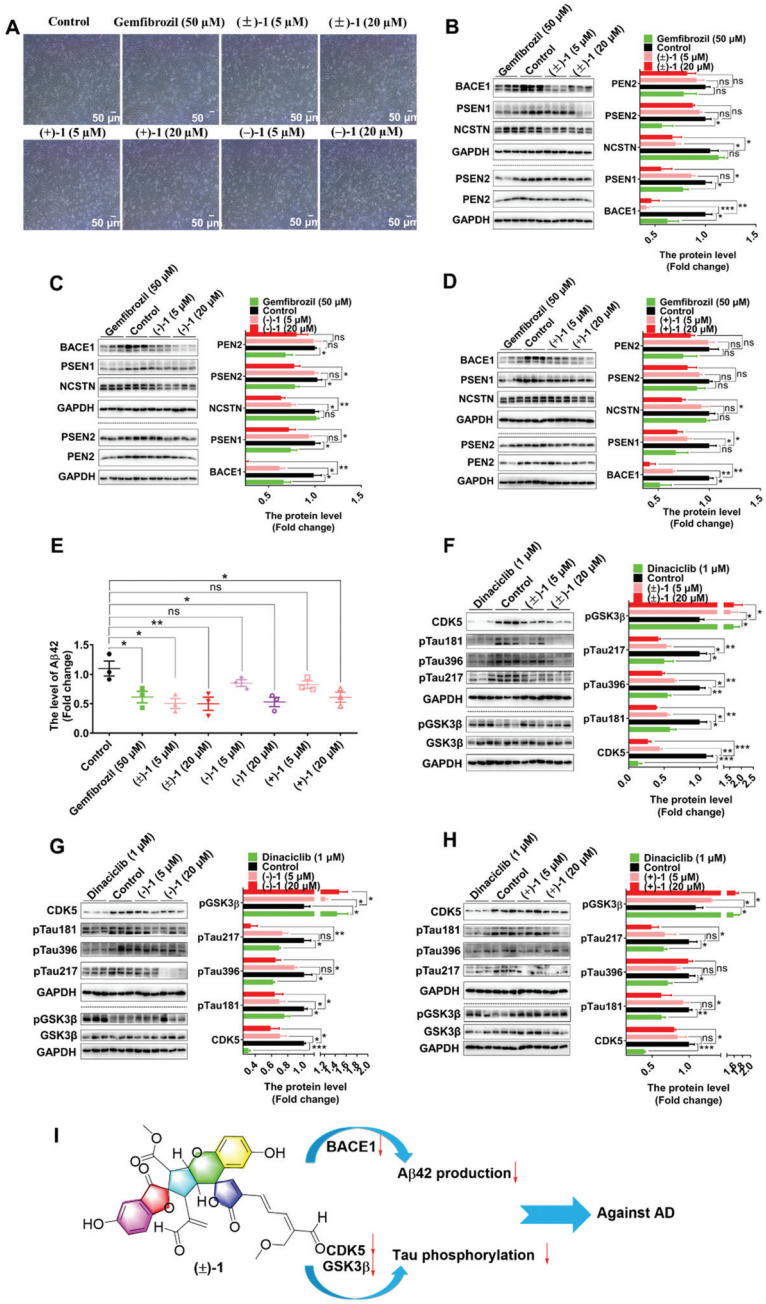

Fig. 4 Results of biological activity assays. (A) The morphology of the U251-APP cells treated with or without compounds (5 μM or 20 μM) or gemfibrozil (50 μM, as a positive control) for 24 h. (B–D) Western blotting assays showing the protein levels of BACE1, NCSTN, PEN2, PSEN1 and PSEN2 in the U251-APP cells treated with or without compounds. A representative western blotting result (left) and quantification of protein levels (right) based on 3 independent experiments. (E) Level of extracellular Aβ42/Aβ1–42 in the supernatant of U251-APP cells treated with compounds or gemfibrozil, or DMSO (control) determined by ELISA. (F–H) Western blotting assays showing the protein levels of CDK5, pGSK3β/GSK3β, pTau396, pTau181 and pTau217 in the U251-APP cells treated with or without compounds, or Dinaciclib (1 μM, as a positive control). A representative western blotting result (left) and quantification of protein levels (right) based on 3 independent experiments. (I) A proposed role of compounds against AD by downregulating BACE1, CDK5 and GSK3β-mediated pathways, resulting in Aβ42 reduction and decreased Tau phosphorylation. Data are presented as the means ± SEM. ns, not significant; ***, $P < 0.001$; **, $P < 0.01$; and *, $P < 0.05$; Student's t test.

Tau (Thr217, pTau217, a new biomarker of AD),[47–49] phospho-Tau (Thr181, pTau181), and phospho-Tau (Ser396, pTau396), which play major roles in the formation of NFT,[10,50] were decreased by (±)-**1**, (+)-**1**, and (−)-**1** treatment. These results also suggest that these compounds can inhibit the phosphorylation of tau and its downstream consequence.

It is worth noting that the above bioassay data showed the inhibition of (±)-**1** against BACE1 at a concentration of 5 μM

was stronger than that at a concentration of 20 μM, while (−)-**1** had stronger inhibitory activity than (+)-**1**. We speculate that (+)-**1** and (−)-**1** can bind with different active sites of BACE1. When the concentration is 5 μM, (+)-**1** and (−)-**1** respectively bind with different active sites, which can result in the increase of inhibition. However, with the increase of concentration, (−)-**1** and (+)-**1** competitively bind to BACE1. It might be that more (−)-**1** finally binds with BACE1 due to the lower binding energy of (−)-**1** (Fig. S18†), leading to the activation of parts of active sites, and a subsequent decrease of inhibition, which will be further confirmed by a competitive experiment.

Conclusions

In conclusion, (±)-spiroganoapplanin A (**1**) is the first example of GMs with a 6/5/5/6/5/6 hexacyclic skeleton from the fruiting bodies of *G. applanatum*. The distinguishing polycyclic structure involves the key Diels–Alder reaction and cyclizations.[26,27,51] Moreover, (±)-**1**, (+)-**1**, and (−)-**1** have potential bioactivity against AD by inhibiting Aβ production and tau phosphorylation in cellular models (Fig. 4I) based on the three lines of evidence: (1) (±)-**1**, (+)-**1**, and (−)-**1** decrease Aβ42 production in U251-APP cells; (2) (±)-**1**, (+)-**1**, and (−)-**1** decrease the protein levels of BACE1, NCSTN and PSEN1; (3) (±)-**1**, (+)-**1**, and (−)-**1** inhibit the protein of CDK5 and the activity of GSK3β, and then inhibit the phosphorylation of tau including pTau181, pTau396, and pTau217. Thus, it would be rewarding to perform focused further studies by testing whether (±)-**1**, (+)-**1**, and (−)-**1** would inhibit the production of Aβ42 and tau hyperphosphorylation, thereby improving the cognitive function in AD animal models.

Experimental section

General experimental procedures

UV spectra were recorded using a Shimadzu UV-2401PC spectrometer. Optical rotations were recorded using a Horiba SEPA-300 polarimeter. CD spectra were recorded using a Chirascan instrument. NMR spectra were recorded using a Bruker AV-600 MHz (Bruker, Zurich, Switzerland) using TMS as an internal standard for chemical shifts. Chemical shifts (δ) were expressed in ppm with reference to the TMS resonance. ESIMS, HRTOF-ESIMS, and UPLC-MS were recorded using an API QSTAR Pulsar spectrometer. A Bruker Tensor-27 instrument by using KBr pellets, and an Agilent 1100 series instrument equipped with an Agilent ZORBAX SB-C18 column (5 μm, 9.6 mm × 250 mm) or a CHIRALCEL OA-H column (5 μm, 4.6 mm × 250 mm) was used for high-performance liquid chromatography (HPLC) analysis and chiral separation, respectively. Silica gel ((200–300) mesh, Qingdao Marine Chemical, Inc.), Lichroprep RP-18 (40–63 μm, Fuji) and Sephadex LH-20 (20–150 μm, Pharmacia) were used for column chromatography. Methanol, chloroform, ethyl acetate, acetone, petroleum ether, *n*-hexane and 2-propanol were purchased from Tianjing Chemical Reagents Co. (Tianjing, China). All other materials were of the highest grade available.

Fungal materials

Ganoderma applanatum (39 kg) was purchased in December 2019 from the traditional Chinese medicine market in Kunming, Yunnan, China, which was identified by Prof. Yang Zhuliang, Kunming Institute of Botany, Chinese Academy of Sciences (voucher No. 19122201).

Extraction and isolation

G. applanatum (39 kg) was chopped and extracted with 95% EtOH under reflux three times (three hours per time). The combined EtOH extracts were evaporated under reduced pressure. The residue was suspended in H_2O and extracted with EtOAc. The volume of the combined EtOAc extracts was reduced to one-third under reduced pressure. The residue was fractionated by macroporous resin (D-101; MeOH–H_2O, 50 : 50, 70 : 30 and 90 : 10, v/v) to yield fractions I–III. Fraction III (158 g) was further fractioned using a silica gel column with $CHCl_3$–MeOH as the mobile phase and gave ten subfractions (Fr. III-1 → Fr. III-10). Fr. III-2 (35 g) was further treated using an Rp-18 column (MeOH–H_2O = 35% → 100%, v/v) to afford eight subfractions. Furthermore, Fr. III-2–4 (5.6 g) were separated using an LH-20 column (MeOH) to give four parts (4a–4d). Then, Fr. III-2–4d (30 mg) were treated and purified by semi-preparative HPLC (CH_3CN–H_2O = 35% containing 0.1% CF_3COOH, v/v, flow rate: 3 mL min^{-1}) to yield compound **1** (12 mg, t_R = 16.8 min).

Compound **1** was isolated as racemates, which were subjected to chiral HPLC (CHIRALCEL OA-H) using *n*-hexane/ethanol (77 : 23, v/v, flow rate: 1 mL min^{-1}) as a mobile phase to yield (−)-**1** (3.8 mg, t_R = 23.7 min) and (+)-**1** (3.5 mg, t_R = 33.1 min).

(±)-Spiroganoapplanin A (1). Yellow crystals (MeOH); {(−)-**1**: $[\alpha]_D^{25}$ −22.1 (*c* 0.10, MeOH), CD (MeOH) Δε214–5.54, Δε253 + 3.90, Δε322–3.34, Δε369 + 1.88; (+)-**1**: $[\alpha]_D^{25}$ +30.0 (*c* 0.11, MeOH), CD (MeOH) Δε213 + 11.0, Δε255–3.28, Δε320 + 4.91, Δε371–1.72}; UV (MeOH) λ_{max} (log ε): 196 (4.64), 258 (4.14), 306 (4.19), and 371 (3.59); IR (KBr) ν_{max} 3450, 2991, 1750, 1530, 1417, 1200 cm^{-1}; ^1H NMR and ^{13}C NMR data: see Table S1;† HRESIMS *m*/*z* 651.1463 $[M + Na]^+$ (calcd for $C_{34}H_{28}O_{12}Na$, 651.1473).

The crystal structure of **1** was solved by direct methods using SHELXS-97 (Sheldrich, G.M. University of Gottingen; Gottingen, Germany, 1997) and the full-matrix least-squares deposited in the Cambridge Crystallographic Data Centre (deposition number: 2098350 for **1**).§

§ **Crystal data for 1**: $C_{34}H_{28}O_{12}\cdot 3(H_2O)$, M = 682.61, a = 9.8432(6) Å, b = 12.6520(8) Å, c = 14.8226(9) Å, α = 66.313(3)°, β = 88.319(3)°, γ = 75.334(3)°, V = 1629.89(18) $Å^3$, T = 100.(2) K, space group $P\bar{1}$, Z = 2, μ(Cu Kα) = 0.937 mm^{-1}, 33527 reflections measured, 6395 independent reflections (R_{int} = 0.0809). The final R_1 values were 0.1125 ($I > 2\sigma(I)$). The final w$R(F^2)$ values were 0.3355 ($I > 2\sigma(I)$). The final R_1 values were 0.1407 (all data). The final w$R(F^2)$ values were 0.3711 (all data). The goodness of fit on F^2 was 1.371.

ECD calculation method for (+)-1 and (−)-1

The theoretical calculations of compound **1** were performed using Gaussian 16.[52] Conformational analysis was carried out. The optimized conformation geometries and thermodynamic parameters of all conformations were provided. The conformers were optimized at the B3LYP/6-311G(d,p) level. The theoretical calculation of ECD was performed using time dependent Density Functional Theory (TDDFT) at the B3LYP/6-311G(d,p) level in MeOH with the PCM model. The ECD spectra of compound **1** were obtained by weighing the Boltzmann distribution rate of each geometric conformation.

Cell culture and treatment

The U251-APP cells were created at the Kunming Institute of Zoology, Chinese Academy of Sciences. The cells were cultured in Roswell RPMI-1640 medium (HyClone, C11875500BT) supplemented with 10% fetal bovine serum (Gibco-BRL, 10099-141) at 37 °C in a humidified atmosphere incubator with 5% CO_2 and 95% humidity, as described in our previous studies.[35–37] The cells were seeded in pre-warmed growth medium in 6-well plates. Chemicals were applied directly to the culture medium for treatment, and the cells were harvested 24 h after treatment.

Western blot analysis

Western blotting for target protein was performed using the common approach as described in our previous studies.[37,41,53] In brief, cell lysates of the U251-APP cells were prepared using the protein lysis buffer (Beyotime Institute of Biotechnology, P0013). The protein concentration was determined using a BCA protein assay kit (Beyotime Institute of Biotechnology, P0012). A total of 20 μg protein was separated by 12% sodium dodecyl sulfate polyacrylamide gel electrophoresis, and was transferred to a polyvinylidene difluoride membrane (Bio-Rad, L1620177 Rev D). The membrane was soaked with 5% (w : v) skim milk for 2 h at room temperature. The membrane was incubated with primary antibodies (GAPDH, glyceraldehyde-3-phosphate dehydrogenase [Proteintech, 60004–1-Ig], BACE1 [Cell Signaling Technology, 5606], PSEN1 [Cell Signaling Technology, 5643], PSEN2 [Cell Signaling Technology, 9979], NICSTN [Cell Signaling Technology, 5665], PEN2 [Cell Signaling Technology, 8598], CDK5 [Santa Cruz Biotechnology, sc-6247], phospho-Tau (Ser396) (pTau396, PHF13) [Cell Signaling Technology, 9632S], phospho-Tau (Thr217) [Abcam, ab192665], phospho-Tau (Thr181) (pTau181) [Cell Signaling Technology, 12885S], phospho-GSK3 β (Ser9) (pGSK3β) [Affinit, AF2016], and GSK-3β (D5C5Z) [Cell Signaling Technology, 12456] overnight at 4 °C. The membranes were washed 3 times with TBST (Tris-buffered saline [Cell Signaling Technology, 9997] with Tween 20 [0.1%; Sigma, P1379]), each time 5 min, followed by incubation with the peroxidase-conjugated anti-mouse (474–1806) or antirabbit (474–1516) IgG (1 : 5000; KPL) for 1 h at room temperature. The epitope was visualized using an ECL western blot detection kit (Millipore, WBKLS0500). ImageJ software (the National Institutes of Health, Bethesda, Maryland, USA) was used to evaluate the densitometry. Western blotting for GAPDH was used as a loading control to measure the densitometry of the target protein.

Aβ ELISA analysis

The level of Aβ42/Aβ1–42 in the supernatant of U251-APP cells was measured using a commercial ELISA kit (Elabscience, E-EL-H0543c), as described in our recent study.[37,41] ELISA was performed for Aβ42 according to the manufacturer's instructions.

Author contributions

X. R. P. and R. C. L. contributed equally to this work. They conducted the main experiments, analysed the data, and wrote the manuscript; M. H. Q. and Y. G. Y. were supervisors for this work and revised the manuscript. X. R. P. finished the ECD calculation. H. G. S., L. Z., X. Q. R., and Y. R. G helped with the experimental procedures. All of the authors reviewed the manuscript.

Conflicts of interest

There are no conflicts to declare.

Acknowledgements

This work was supported by grants from the Basic Research Program of Yunnan Province (202001AT070070 to X. R. P., and 202201AW070010 and 202001AT070107 to R. C. L.), the Youth Innovation Promotion Association of CAS (2019383 to X. R. P. and 2021000011 to R. C. L.), the National Natural Science Foundation of China (31730037 to Y. G. Y., 32170988 and 31900737 to R. C. L.), the Original Innovation Project "from 0 to 1" of the Basic Frontier Scientific Research Program, CAS (ZDBS-LY-SM031 to R. C. L.), the Strategic Priority Research Program (B) of CAS (XDB02020003 to Y. G. Y.), the CAS "Light of West China" Program (2020000023 to R. C. L.) and the Young Scientific and Technological Talents Promotion Project of Yunnan Association for Science and Technology (2022000043 to R. C. L). The authors are grateful to the Analytical and Testing Center at Kunming Institute of Botany for NMR and ECD data collection.

Notes and references

1 Alzheimer's Association, 2015 Alzheimer's disease facts and figures, *Alzheimer's Dementia*, 2015, **11**, 332–384.
2 P. Scheltens, B. De Strooper, M. Kivipelto, H. Holstege, G. Chételat, C. E. Teunissen, J. Cummings and W. M. van der Flier, Alzheimer's disease, *Lancet*, 2021, **397**, 1577–1590.
3 H. Malkki, Alzheimer disease: NGF gene therapy activates neurons in the AD patient brain, *Nat. Rev. Neurol.*, 2015, **11**, 548.

4 M. A. Busche and B. T. Hyman, Synergy between amyloid-beta and tau in Alzheimer's disease, *Nat. Neurosci.*, 2020, **23**, 1183–1193.
5 A. Baker-Nigh, S. Vahedi, E. G. Davis, S. Weintraub, E. H. Bigio, W. L. Klein and C. Geula, Neuronal amyloid-beta accumulation within cholinergic basal forebrain in ageing and Alzheimer's disease, *Brain*, 2015, **138**, 1722–1737.
6 T. Silva, J. Teixeira, F. Remiao and F. Borges, Alzheimer's disease, cholesterol, and statins: the junctions of important metabolic pathways, *Angew. Chem., Int. Ed.*, 2013, **52**, 1110–1121.
7 D. Alcolea, P. Martínez-Lage, P. Sánchez-Juan, J. Olazarán, C. Antúnez, A. Izagirre, M. Ecay-Torres, A. Estanga, M. Clerigué, M. C. Guisasola, D. Sánchez Ruiz, J. Marín Muñoz, M. Calero, R. Blesa, J. Clarimón, M. Carmona-Iragui, E. Morenas-Rodríguez, E. Rodríguez-Rodríguez, J. L. Vázquez Higuera, J. Fortea and A. Lleó, Amyloid precursor protein metabolism and inflammation markers in preclinical Alzheimer disease, *Neurology*, 2015, **85**, 626–659.
8 A. K. Ghosh and H. L. Osswald, BACE1 (β-secretase) inhibitors for the treatment of Alzheimer's disease, *Chem. Soc. Rev.*, 2014, **43**, 6765–6813.
9 E. E. Congdon and E. M. Sigurdsson, Tau-targeting therapies for Alzheimer disease, *Nat. Rev. Neurol.*, 2018, **14**, 399–415.
10 C. Li and J. Gotz, Tau-based therapies in neurodegeneration: opportunities and challenges, *Nat. Rev. Drug Discovery*, 2017, **16**, 863–883.
11 O. Benek, J. Korabecny and O. Soukup, A perspective on multi-target drugs for Alzheimer's disease, *Trends Pharmacol. Sci.*, 2020, **41**, 434–445.
12 H. H. Peng, C. Y. Wu, Y. C. Hsiao, J. Martel, P. Y. Ke, C. Y. Chiu, J. C. Liau, I. T. Chang, Y. H. Su, Y. F. Ko, J. D. Young and D. M. Ojcius, *Ganoderma lucidum* stimulates autophagy-dependent longevity pathways in *Caenorhabditis elegans* and human cells, *Aging*, 2021, **13**, 13474–13495.
13 R. W. Kou, Y. Q. Gao, B. Xia, J. Y. Wang, X. N. Liu, J. J. Tang, X. Yin and J. M. Gao, Ganoderterpene A, a new triterpenoid from *Ganoderma lucidum*, attenuates LPS-induced inflammation and apoptosis via suppressing MAPK and TLR-4/NF-kappaB pathways in BV-2 cells, *J. Agric. Food Chem.*, 2021, **69**, 12730–12740.
14 A. Hilliard, P. Mendonca and K. F. A. Soliman, Involvement of NFkB and MAPK signaling pathways in the preventive effects of *Ganoderma lucidum* on the inflammation of BV-2 microglial cells induced by LPS, *J. Neuroimmunol.*, 2020, **345**, 577269–577278.
15 C. Zhao, C. Zhang, Z. Xing, Z. Ahmad, J. S. Li and M. W. Chang, Pharmacological effects of natural *Ganoderma* and its extracts on neurological diseases: A comprehensive review, *Int. J. Biol. Macromol.*, 2019, **121**, 1160–1178.
16 Z. M. Jiang, H. B. Qiu, S. Q. Wang, J. Guo, Z. W. Yang and S. B. Zhou, Ganoderic acid A potentiates the antioxidant effect and protection of mitochondrial membranes and reduces the apoptosis rate in primary hippocampal neurons in magnesium free medium, *Pharmazie*, 2018, **73**, 87–91.
17 P. Sharma and R. Tulsawani, *Ganoderma lucidum* aqueous extract prevents hypobaric hypoxia induced memory deficit by modulating neurotransmission, neuroplasticity and maintaining redox homeostasis, *Sci. Rep.*, 2020, **10**, 8944–8970.
18 L. F. Qi, S. Liu, Y. C. Liu, P. Li and X. Xu, Ganoderic Acid A promotes amyloid-beta clearance (*in vitro*) and ameliorates cognitive deficiency in Alzheimer's disease (mouse model) through autophagy induced by activating Axl, *Int. J. Mol. Sci.*, 2021, **22**, 5559–5577.
19 J.-J. Zhang, Y. Dong, F.-Y. Qin and Y.-X. Cheng, Australeols A-F, neuroprotective meroterpenoids from *Ganoderma australe*, *Fitoterapia*, 2019, **134**, 250–255.
20 H. Chen, J. Zhang, J. Ren, W. Wang, W. Xiong, Y. Zhang, L. Bao and H. Liu, Triterpenes and meroterpenes with neuroprotective effects from *Ganoderma leucocontextum*, *Chem. Biodivers.*, 2018, **15**, e1700567–e1700576.
21 X. H. Tang, R. C. Luo, M. S. Ye, H. Y. Tang, Y. L. Ma, Y. N. Chen, X. M. Wang, Q. Y. Lu, S. Liu, X. N. Li, Y. Yan, J. Yang, X. Q. Ran, X. Fang, Y. Zhou, Y. G. Yao, Y. T. Di and X. J. Hao, Harpertrioate A, an A,B,D-seco-Limonoid with promising biological activity against Alzheimer's disease from twigs of *Harrisonia perforat*a, (Blanco) Merr, *Org. Lett.*, 2021, **23**, 262–267.
22 C. A. Schmidt, R. Murillo, B. Heinzmann, S. Laufer, V. Wray and I. Merfort, Structural and conformational analysis of proanthocyanidins from *Parapiptadenia rigida* and their wound-healing properties, *J. Nat. Prod.*, 2011, **74**, 1427–1436.
23 M. Esposito, L. F. Nothias, H. Nedev, J. F. Gallard, P. Leyssen, P. Retailleau, J. Costa, F. Roussi, B. I. Iorga, J. Paolini and M. Litaudon, *Euphorbia dendroides* Latex as a source of jatrophane esters: isolation, structural analysis, conformational study, and anti-CHIKV activity, *J. Nat. Prod.*, 2016, **79**, 2873–2882.
24 L. C. Forster, G. K. Pierens, J. K. Clegg and M. J. Garson, Dynamic NMR and computational studies inform the conformational description of dendrillane terpenes from the Nudibranch *Goniobranchus coi*, *J. Nat. Prod.*, 2020, **83**, 714–719.
25 B. Liu, S. Fu and C. Zhou, Naturally occurring [4+2] type terpenoid dimers: sources, bioactivities and total syntheses, *Nat. Prod. Rep.*, 2020, **37**, 1627–1660.
26 X. R. Peng, Q. Wang, H. R. Wang, K. Hu, W. Y. Xiong and M. H. Qiu, FPR2-based anti-inflammatory and anti-lipogenesis activities of novel meroterpenoid dimers from *Ganoderma*, *Bioorg. Chem.*, 2021, **116**, 105338–105348.
27 X. Peng, H. Su, H. Wang, G. Hu, K. Hu, L. Zhou and M. Qiu, Applanmerotic acids A and B, two meroterpenoid dimers with an unprecedented polycyclic skeleton from

Ganoderma applanatum that inhibit formyl peptide receptor 2, *Org. Chem. Front.*, 2021, **8**, 3381–3389.

28 F. Y. Qin, H. X. Zhang, Q. Q. Di, Y. Wang, Y. M. Yan, W. L. Chen and Y. X. Cheng, *Ganoderma cochlear* metabolites as probes to identify a COX-2 active site and as in vitro and in vivo anti-inflammatory agents, *Org. Lett.*, 2020, **22**, 2574–2578.

29 F. J. Zhou, Y. Nian, Y. Yan, Y. Gong, Q. Luo, Y. Zhang, B. Hou, Z. L. Zuo, S. M. Wang, H. H. Jiang, J. Yang and Y. X. Cheng, Two new classes of T-type calcium channel inhibitors with new chemical scaffolds from *Ganoderma cochlear*, *Org. Lett.*, 2015, **17**, 3082–3085.

30 Q. Luo, L. Di, W. F. Dai, Q. Lu, Y. M. Yan, Z. L. Yang, R. T. Li and Y. X. Cheng, Applanatumin A, a new dimeric meroterpenoid from *Ganoderma applanatum* that displays potent antifibrotic activity, *Org. Lett.*, 2015, **17**, 1110–1113.

31 Q. Luo, Z. Wang, J. F. Luo, Z. C. Tu and Y. X. Cheng, (±)-Applanatumines B–D: novel dimeric meroterpenoids from *Ganoderma applanatum* as inhibitors of JAK3, *RSC Adv.*, 2017, **7**, 38037–38043.

32 T. Yang, L. Zhang, Y. Shang, Z. Zhu, S. Jin, Z. Guo and X. Wang, Concurrent suppression of Aβ aggregation and NLRP3 inflammasome activation for treating Alzheimer's disease, *Chem. Sci.*, 2022, **13**, 2971–2980.

33 X. Peng, J. Liu, C. Wang, Z. Han, Y. Shu, X. Li, L. Zhou and M. Qiu, Unusual prenylated phenols with antioxidant activities from *Ganoderma cochlear*, *Food Chem.*, 2015, **171**, 251–257.

34 S. Y. Lu, X. R. Peng, J.R. Dong, H. Yan, Q. H. Kong, Q. Q. Shi, D. S. Li, L. Zhou, Z. R. Li and M. H. Qiu, Aromatic constituents from *Ganoderma lucidum* and their neuroprotective and anti-inflammatory activities, *Fitoterapia*, 2019, **134**, 58–64.

35 Q. Xiang, R. Bi, M. Xu, D. F. Zhang, L. W. Tan, C. Zhang, Y. R. Fang and Y. G. Yao, Rare genetic variants of the transthyretin gene are associated with Alzheimer's disease in Han Chinese, *Mol. Neurobiol.*, 2017, **54**, 5192–5200.

36 D. F. Zhang, J. Li, H. Wu, Y. Cui, R. Bi, H. J. Zhou, H. Z. Wang, C. Zhang, D. Wang, Alzheimer's Disease Neuroimaging Initiative (ADNI), Q. P. Kong, T. Li, Y. R. Fang, T. Z. Jiang and Y. G. Yao, CFH variants affect structural and functional brain changes and genetic risk of Alzheimer's disease, *Neuropsychopharmacology*, 2016, **41**, 1034–1045.

37 R. Luo, Y. Fan, J. Yang, M. Ye, D. F. Zhang, K. Guo, X. Li, R. Bi, M. Xu, L. X. Yang, Y. Li, X. Ran, H. Y. Jiang, C. Zhang, L. Tan, N. Sheng and Y. G. Yao, A novel missense variant in ACAA1 contributes to early-onset Alzheimer's disease, impairs lysosomal function, and facilitates amyloid-beta pathology and cognitive decline, *Signal Transduction Targeted Ther.*, 2021, **6**, 325–341.

38 H. B. Rubins, S. J. Robins, D. Collins, C. L. Fye, J. W. Anderson, M. B. Elam, F. H. Faas, E. Linares, E. J. Schaefer, G. Schectman, T. J. Wilt and J. Wittes, Gemfibrozil for the secondary prevention of coronary heart disease in men with low levels of high-density lipoprotein cholesterol. Veterans affairs high-density lipoprotein cholesterol intervention trial Study group, *N. Engl. J. Med.*, 1999, **341**, 410–418.

39 M. H. Frick, O. Elo, K. Haapa, O. P. Heinonen, P. Heinsalmi, P. Helo, J. K. Huttunen, P. Kaitaniemi, P. Koskinen, V. Manninen, *et al.*, Helsinki heart study: primary-prevention trial with gemfibrozil in middle-aged men with dyslipidemia. Safety of treatment, changes in risk factors, and incidence of coronary heart disease, *N. Engl. J. Med.*, 1987, **317**, 1237–1245.

40 G. T. Corbett, F. J. Gonzalez and K. Pahan, Activation of peroxisome proliferator-activated receptor alpha stimulates ADAM10-mediated proteolysis of APP, *Proc. Natl. Acad. Sci. U. S. A.*, 2015, **112**, 8445–8450.

41 R. Luo, L. Y. Su, G. Li, J. Yang, Q. Liu, L. X. Yang, D. F. Zhang, H. Zhou, M. Xu, Y. Fan, J. Li and Y. G. Yao, Activation of PPARA-mediated autophagy reduces Alzheimer disease-like pathology and cognitive decline in a murine model, *Autophagy*, 2020, **16**, 52–69.

42 H. W. Querfurth and F. M. LaFerla, Alzheimer's disease, *N. Engl. J. Med.*, 2010, **362**, 329–344.

43 R. Vassar, B. D. Bennett, S. Babu-Khan, S. Kahn, E. A. Mendiaz, P. Denis, D. B. Teplow, S. Ross, P. Amarante, R. Loeloff, Y. Luo, S. Fisher, L. Fuller, S. Edenson, J. Lile, M. A. Jarosinski, A. L. Biere, E. Curran, T. Burgess, J. C. Louis, F. Collins, J. Treanor, G. Rogers and M. Citron, beta-secretase cleavage of Alzheimer's amyloid precursor protein by the transmembrane aspartic protease BACE, *Science*, 1999, **286**, 735–741.

44 L. Mucke and D. J. Selkoe, Neurotoxicity of amyloid beta-protein: synaptic and network dysfunction, *Cold Spring Harbor Perspect. Med.*, 2012, **2**, 17.

45 S. K. Kumar, B. LaPlant, W. J. Chng, J. Zonder, N. Callander, R. Fonseca, B. Fruth, V. Roy, C. Erlichman, A. K. Stewart and C. Mayo Phase, Dinaciclib, a novel CDK inhibitor, demonstrates encouraging single-agent activity in patients with relapsed multiple myeloma, *Blood*, 2015, **125**, 443–448.

46 D. A. Cross, D. R. Alessi, P. Cohen, M. Andjelkovich and B. A. Hemmings, Inhibition of glycogen synthase kinase-3 by insulin mediated by protein kinase B, *Nature*, 1995, **378**, 785–789.

47 S. Janelidze, E. Stomrud, R. Smith, S. Palmqvist, N. Mattsson, D. C. Airey, N. K. Proctor, X. Y. Chai, S. Shcherbinin, J. R. Sims, G. Triana-Baltzer, C. Theunis, R. Slemmon, M. Mercken, H. Kolb, J. L. Dage and O. Hansson, Cerebrospinal fluid p-tau217 performs better than p-tau181 as a biomarker of Alzheimer's disease, *Nat. Commun.*, 2020, **11**, 1683–1695.

48 N. Mattsson-Carlgren, S. Janelidze, S. Palmqvist, N. Cullen, A. L. Svenningsson, O. Strandberg, D. Mengel, D. M. Walsh, E. Stomrud, J. L. Dage and O. Hansson, Longitudinal plasma p-tau217 is increased in early stages of Alzheimer's disease, *Brain*, 2020, **143**, 3234–3241.

49 S. Palmqvist, S. Janelidze, Y. T. Quiroz, H. Zetterberg, F. Lopera, E. Stomrud, Y. Su, Y. H. Chen, G. E. Serrano,

A. Leuzy, N. Mattsson-Carlgren, O. Strandberg, R. Smith, A. Villegas, D. Sepulveda-Falla, X. Y. Chai, N. K. Proctor, T. G. Beach, K. Blennow, J. L. Dage, E. M. Reiman and O. Hansson, Discriminative accuracy of plasma phospho-tau217 for Alzheimer disease vs other neurodegenerative disorders, *JAMA*, 2020, **324**, 772–781.

50 S. Stathas, V. E. Alvarez, W. Xia, R. Nicks, G. Meng, S. Daley, M. Pothast, A. Shah, H. Kelley, C. Esnault, R. McCormack, E. Dixon, L. Fishbein, J. D. Cherry, B. R. Huber, Y. Tripodis, M. L. Alosco, J. Mez, A. C. McKee and T. D. Stein, Tau phosphorylation sites serine202 and serine396 are differently altered in chronic traumatic encephalopathy and Alzheimer's disease, *Alzheimers Dement*, 2021, DOI: **10.1002/alz.12502**.

51 X. Peng and M. Qiu, Meroterpenoids from *Ganoderma* species: a review of last five years, *Nat. Prod. Bioprospect.*, 2018, **8**, 137–149.

52 M. Srebro-Hooper and J. Autschbach, Calculating natural optical activity of molecules from first principles, *Annu. Rev. Phys. Chem.*, 2017, **68**, 399–420.

53 L. Y. Su, R. Luo, Q. Liu, J. R. Su, L. X. Yang, Y. Q. Ding, L. Xu and Y. G. Yao, Atg5- and Atg7-dependent autophagy in dopaminergic neurons regulates cellular and behavioral responses to morphine, *Autophagy*, 2017, **13**, 1496–1511.

Electronic Supplementary Material (ESI) for Organic Chemistry Frontiers.

(±)-Spiroganoapplanin A, a complex polycyclic meroterpenoid dimer from *Ganoderma applanatum* displaying the potential against Alzheimer's disease

Xing-Rong Peng,[a,c,‡] Rong-Can Luo,[b,c,‡] Hai-Guo Su,[a] Lin Zhou,[a] Xiao-Qian Ran,[b,c] Ya-Rong Guo,[d] Yong-Gang Yao,[b,c,e,*] Ming-Hua Qiu[a,c,*]

[a] State Key Laboratory of Phytochemistry and Plant Resources in West China, Kunming Institute of Botany, Chinese Academy of Science, Kunming 650201, China

[b] Kunming College of Life Science, University of Chinese Academy of Sciences, Kunming, Yunnan 650204, China

[c] Key Laboratory of Animal Models and Human Disease Mechanisms of the Chinese Academy of Sciences & Yunnan Province, KIZ-CUHK Joint Laboratory of Bioresources and Molecular Research in Common Diseases, Kunming Institute of Zoology, Chinese Academy of Sciences, Kunming 650204, China

[d] School of Life Sciences, Division of Life Sciences and Medicine, University of Science and Technology of China, Hefei 230026, China

[e] CAS Center for Excellence in Brain Science and Intelligence Technology, Chinese Academy of Sciences, Shanghai 200031, China

[‡]These authors equally contributed to this work.

Contents

Table S1. ^{1}H and ^{13}C NMR Spectroscopic Data (Methanol-d_4) of (±)-1. (δ in *ppm*)

No.	$^{1}H^{a}$ (J in Hz)	$^{13}C^{a}$	$^{1}H^{b}$ (J in Hz)	$^{13}C^{b}$
1a		166.6 C		165.5 C
2a		121.9 C		120.7 C
3a	6.80, d (2.7)	107.9 CH	6.64, d (2.7)	106.2 CH
4a		154.5 C		152.0 C
5a	7.14, dd (8.9, 2.7)	129.0 CH	7.04, dd (8.9, 2.7)	127.6 CH
6a	6.92, d (8.9)	114.7 CH	6.84, d (8.9)	113.5 CH
7a		n.o.		200.2 C
8a		n.o.		91.3 C
9a	3.82, d (9.7)	56.9 CH	3.76, d (9.4)	55.2 CH
10a	4.85, br s	76.7 CH	4.78 m	75.1 CH
11a	n.o.	n.o.	3.47 m	45.8 CH
12a	n.o.	n.o.	3.18 overlapped	42.8 CH
13a		143.1 C		141.6 C
14a	n.o.	n.o.	6.35, s; 6.76, s	142.3 CH_2
15a	n.o.	n.o.	8.95, s	192.5 CH
16a		170.1 C		170.5 C
17a	3.50, s	52.6 CH_3	3.43, s	51.4 CH_3
1b		153.3 C		151.2 C
2b		120.5 C		119.2 C
3b	6.30, d (2.9)	112.5 CH	6.18, d (2.8)	111.0 CH
4b		149.5 C		148.1 C
5b	6.75, dd (9.0, 2.9)	119.5 CH	6.65, dd (8.9, 2.8)	118.0 CH
6b	6.84, d (9.0)	119.8 CH	6.75, d (8.9)	118.5 CH
7b		87.5 C		86.2 C
8b	8.05, s	154.0 CH	8.02, s	153.3 CH
9b		129.8 C		128.2 C
10b	6.83, overlapped	130.7 CH	6.74, overlapped	129.5 CH
11b	7.89, dd (15.6, 11.6)	131.4 CH	7.81, dd (15.2, 11.4)	130.0 CH
12b	7.22, d (11.6)	152.1 CH	7.15, d (11.6)	151.3 CH
13b		140.5 C		139.1 C
14b	4.25, d (3.7)	64.4 CH_2	4.14, d (1.9)	62.8 CH_2
15b	9.49, s	195.2 CH	9.39, s	194.3 CH
16b		171.7 C		170.5 C
17b	3.32, s	58.7 CH_3	3.21, s	57.6 CH_3

[a]: 600/150 MHz, 298 K; [b]: 400/100 MHz, 253 K; n.o.: no signal

1D and 2D NMR spectra of compound 1 (298 K)

Figure S1. ^{1}H NMR (600 MHz, CD_3OD) spectrum of 1.

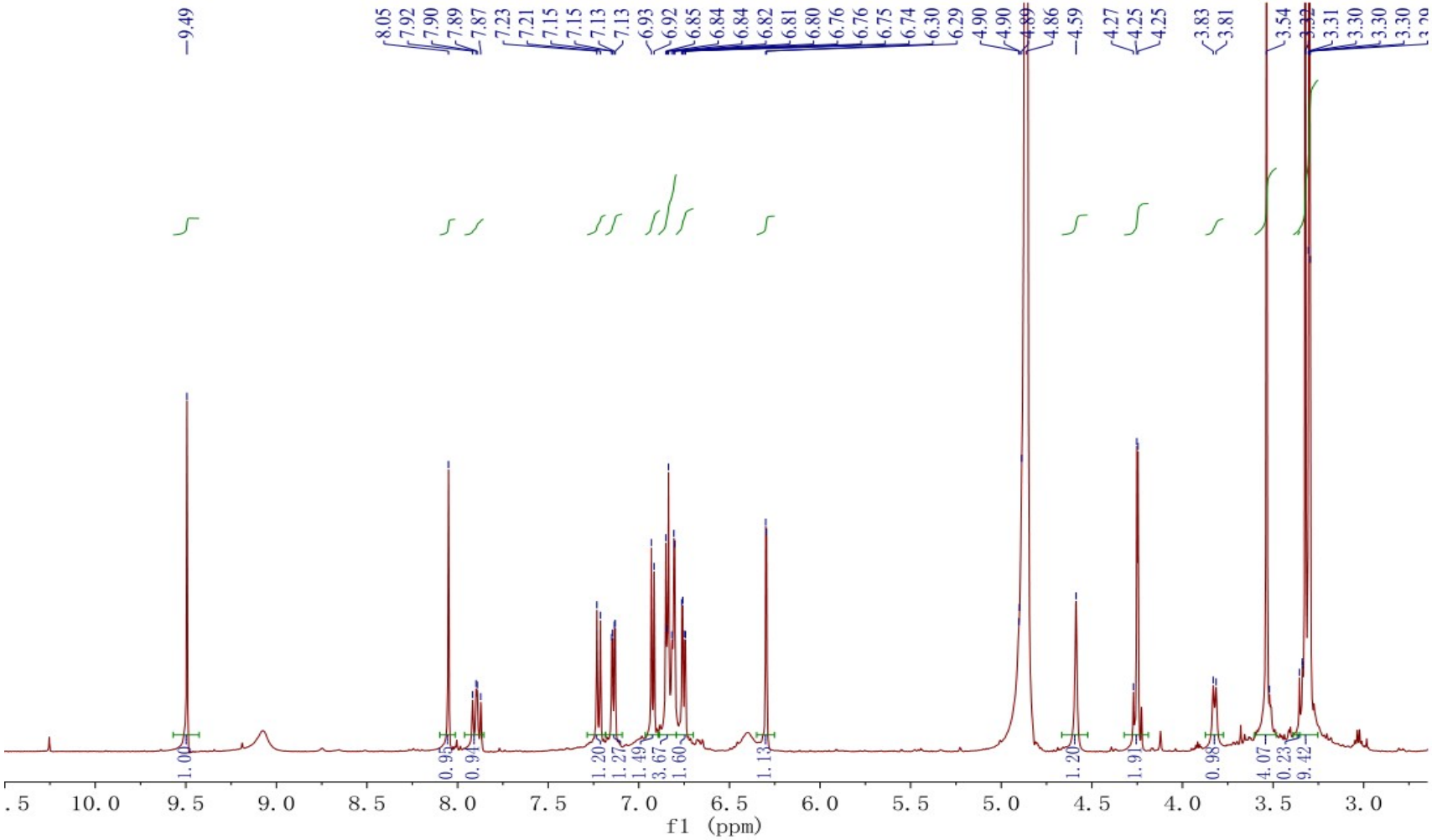

Figure S2. ^{13}C NMR (150 MHz, CD_3OD) spectrum of 1.

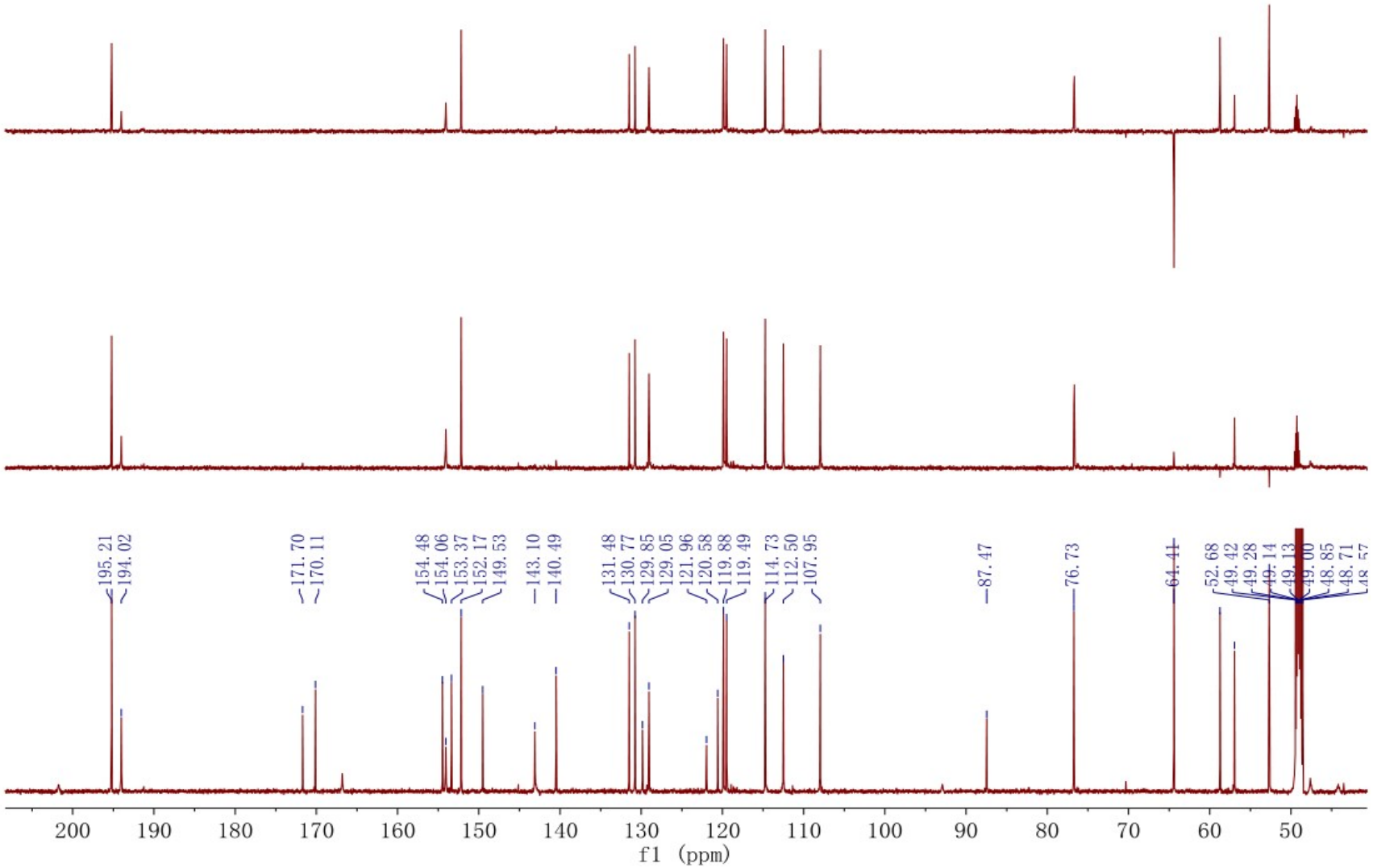

Figure S3. ^{1}H-^{1}H COSY (600 MHz, CD_3OD) spectrum of 1.

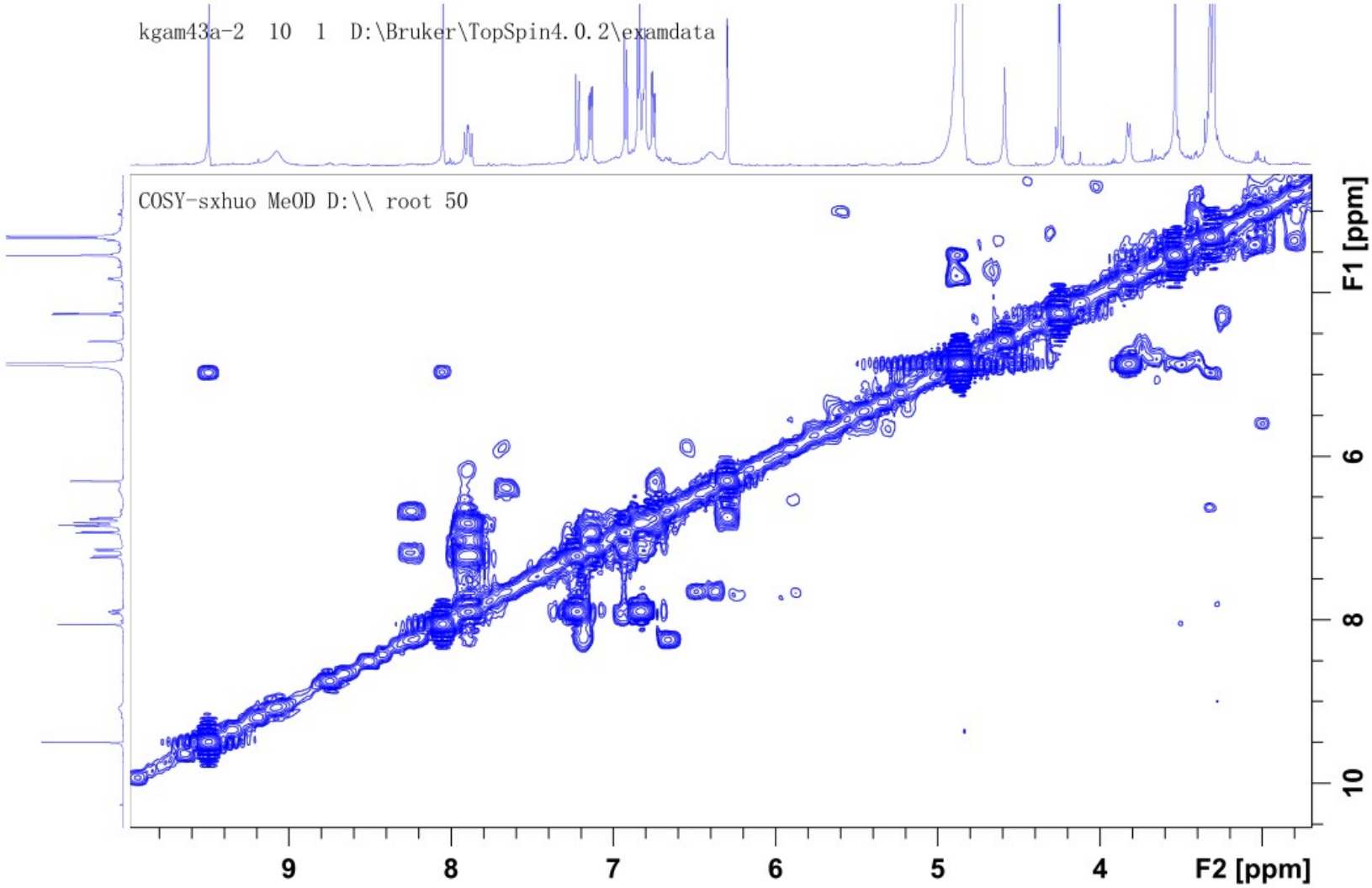

Figure S4. HSQC (600/150 MHz, CD_3OD) spectrum of 1.

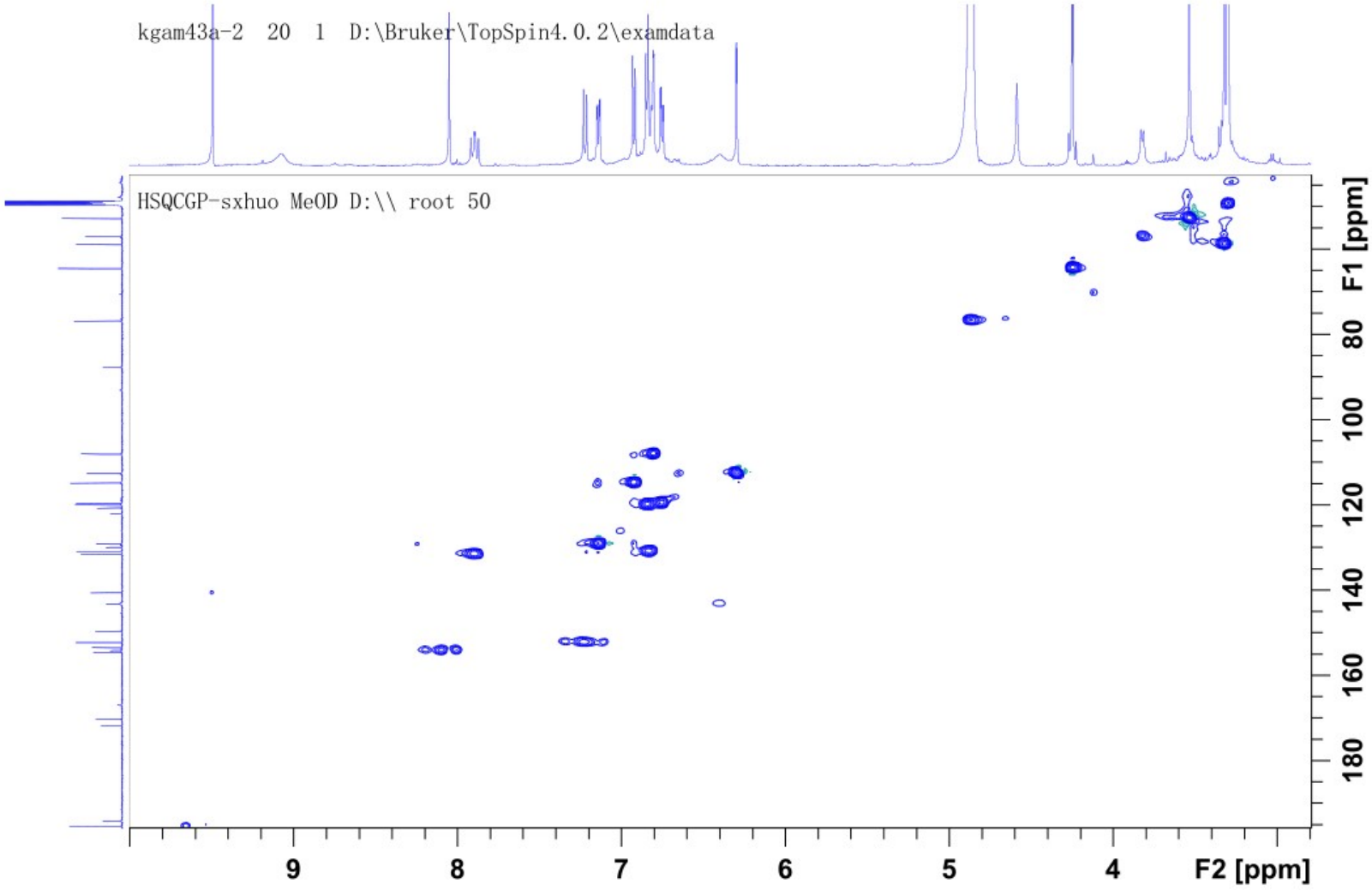

Figure S5. HMBC (600/150 MHz, CD_3OD) spectrum of 1.

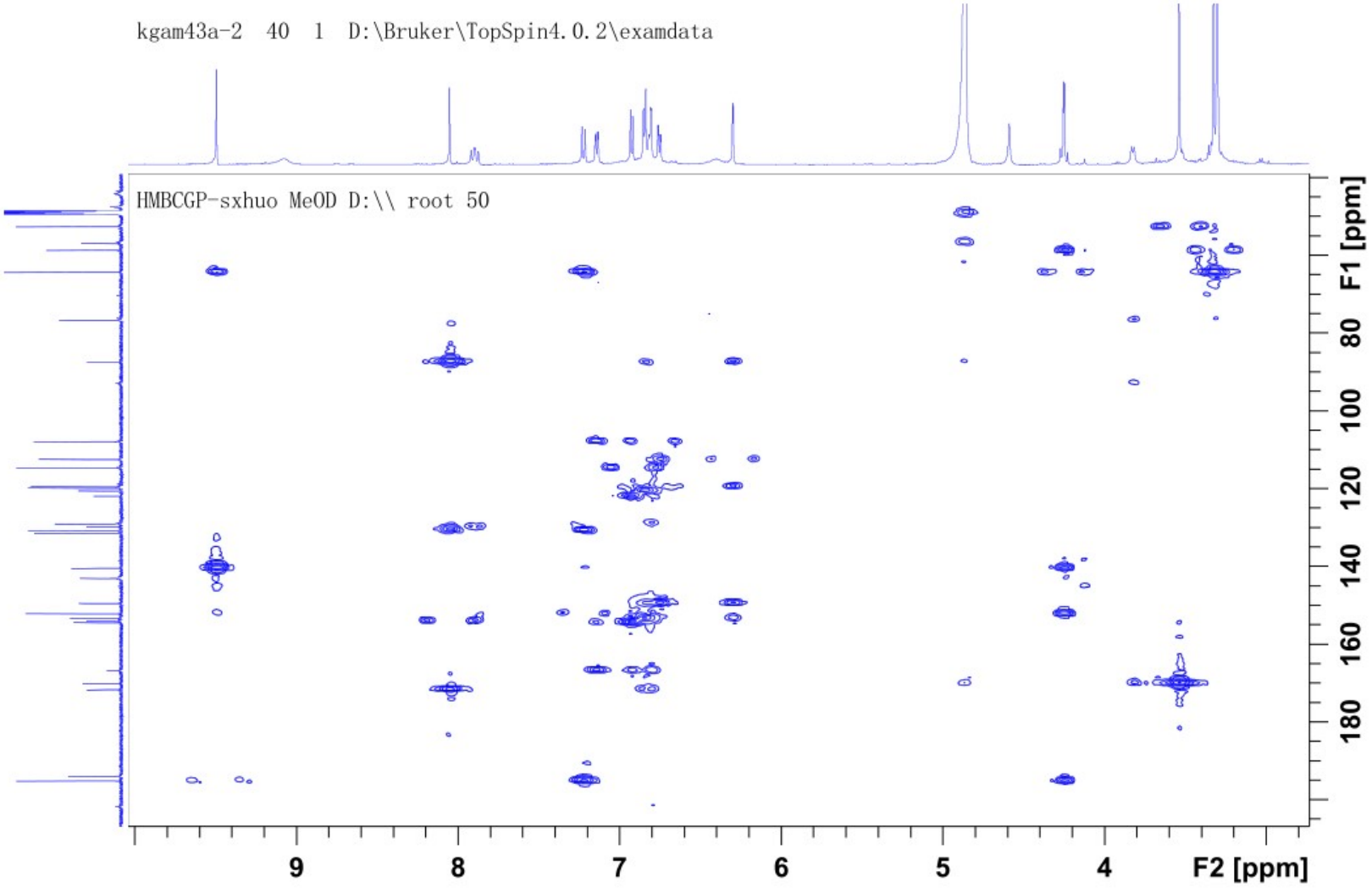

Figure S6. ROESY (600 MHz, CD_3OD) spectrum of 1.

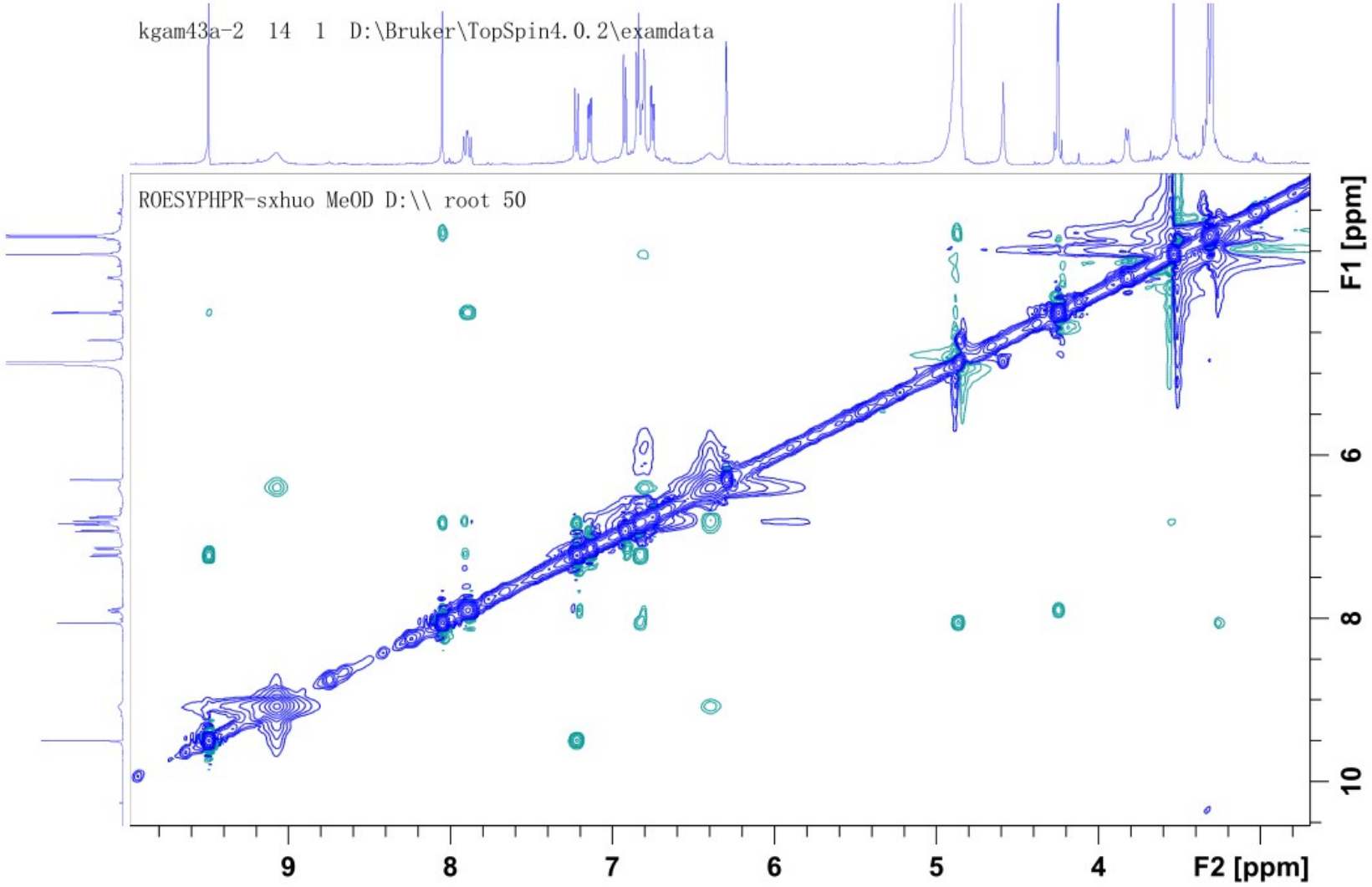

1D and 2D NMR spectra of compound 1 (253 K)

Figure S7. ^{1}H NMR (400 MHz, CD_3OD) spectrum of 1.

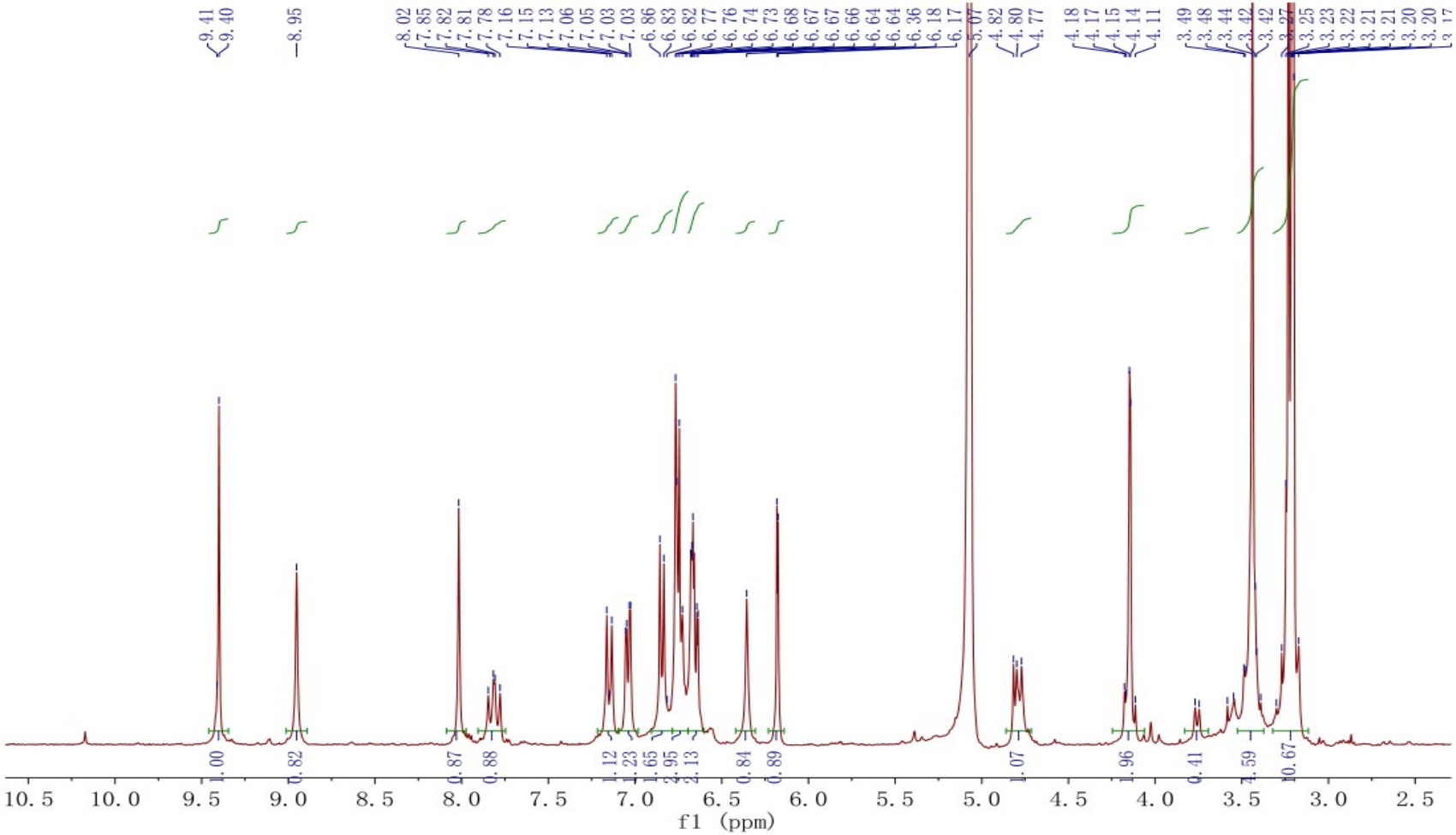

Figure S8. The comparison of the ^{1}H NMR (400 MHz, CD_3OD) spectra of 1 at variational temperature.

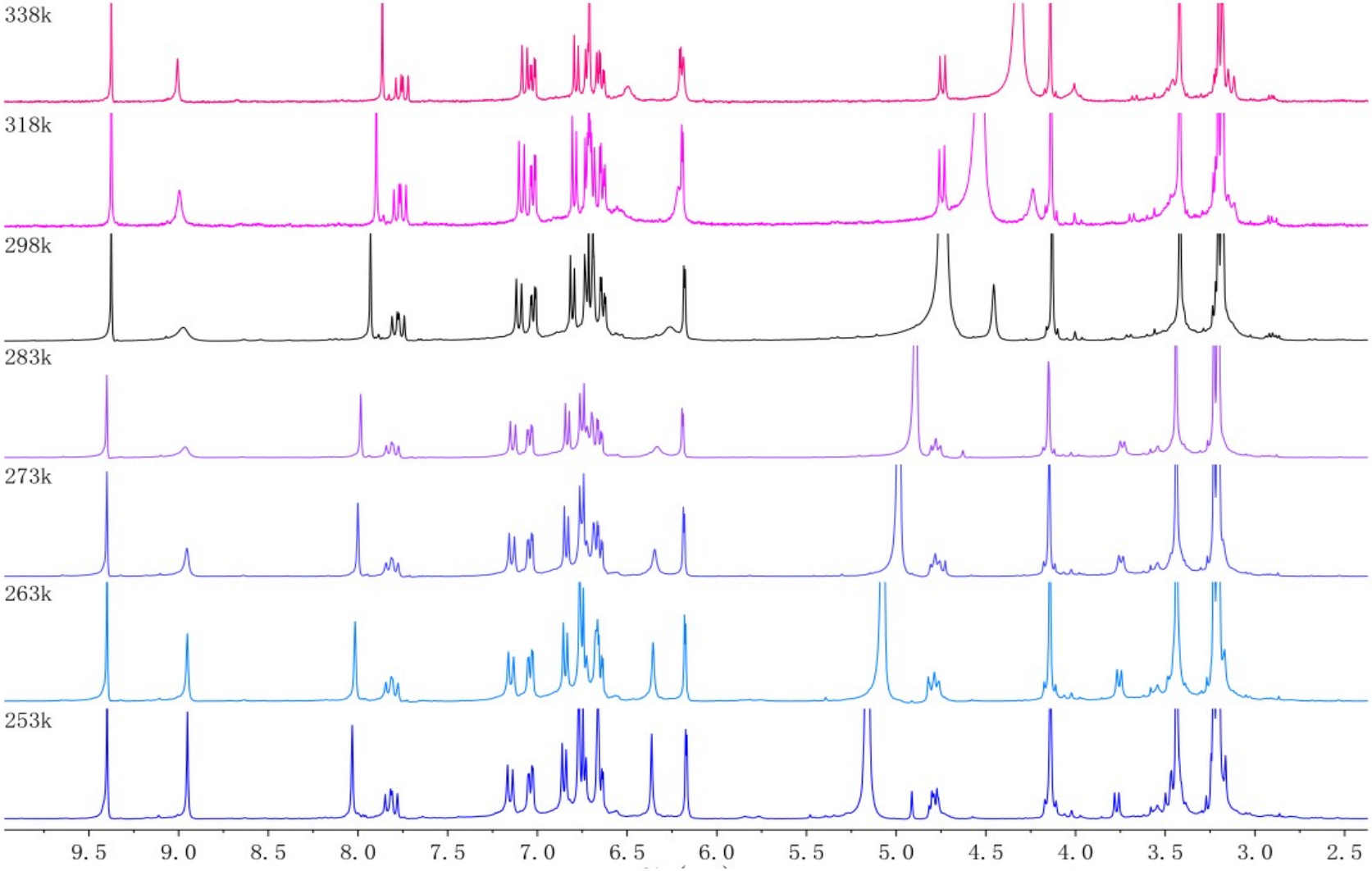

Figure S9. ^{13}C NMR (100 MHz, CD_3OD) spectrum of 1.

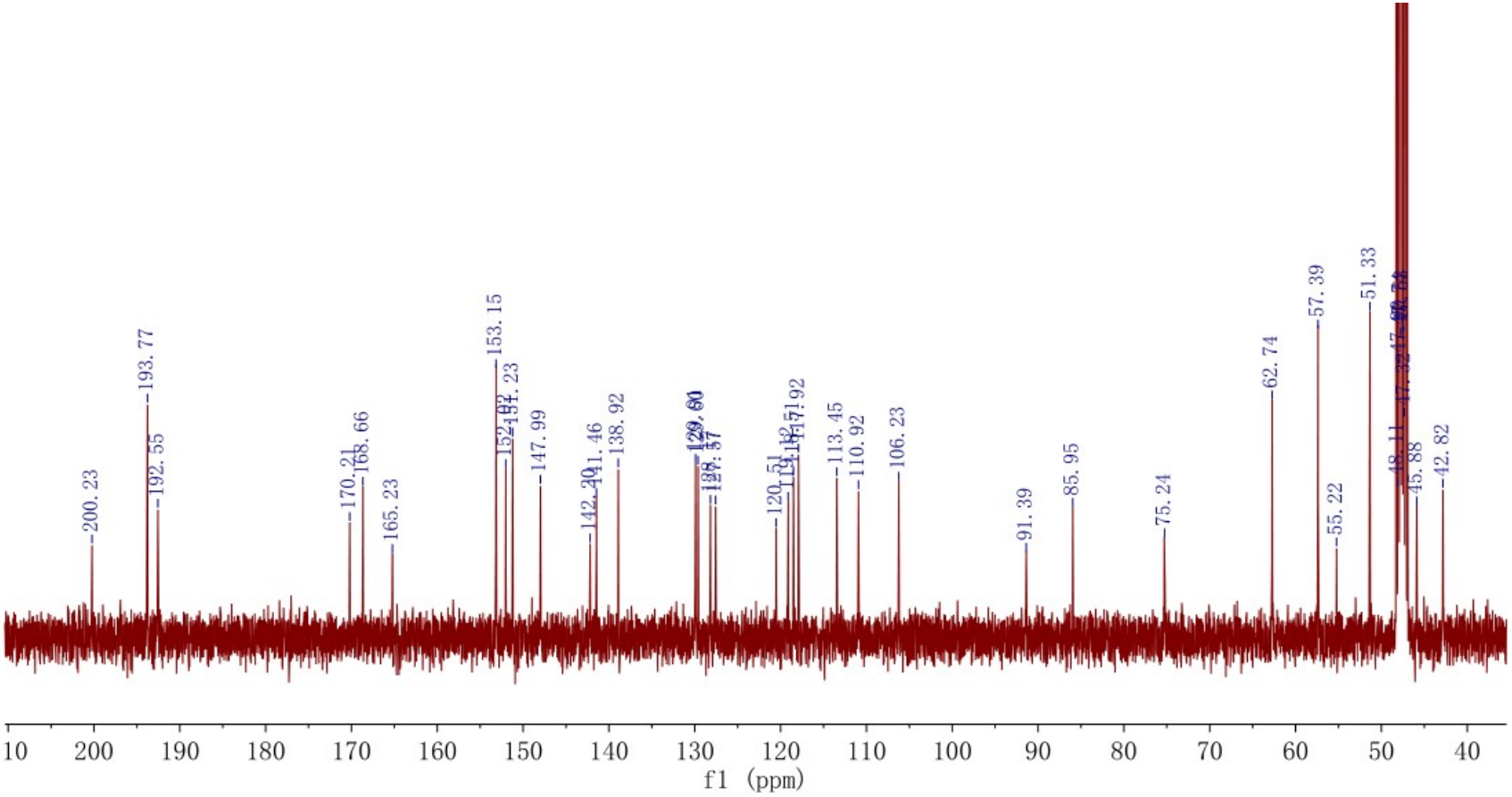

Figure S10. The comparison of the ^{13}C NMR spectra of 1 at 298 K (150 MHz, CD_3OD) and 253 K (100 MHz, CD_3OD).

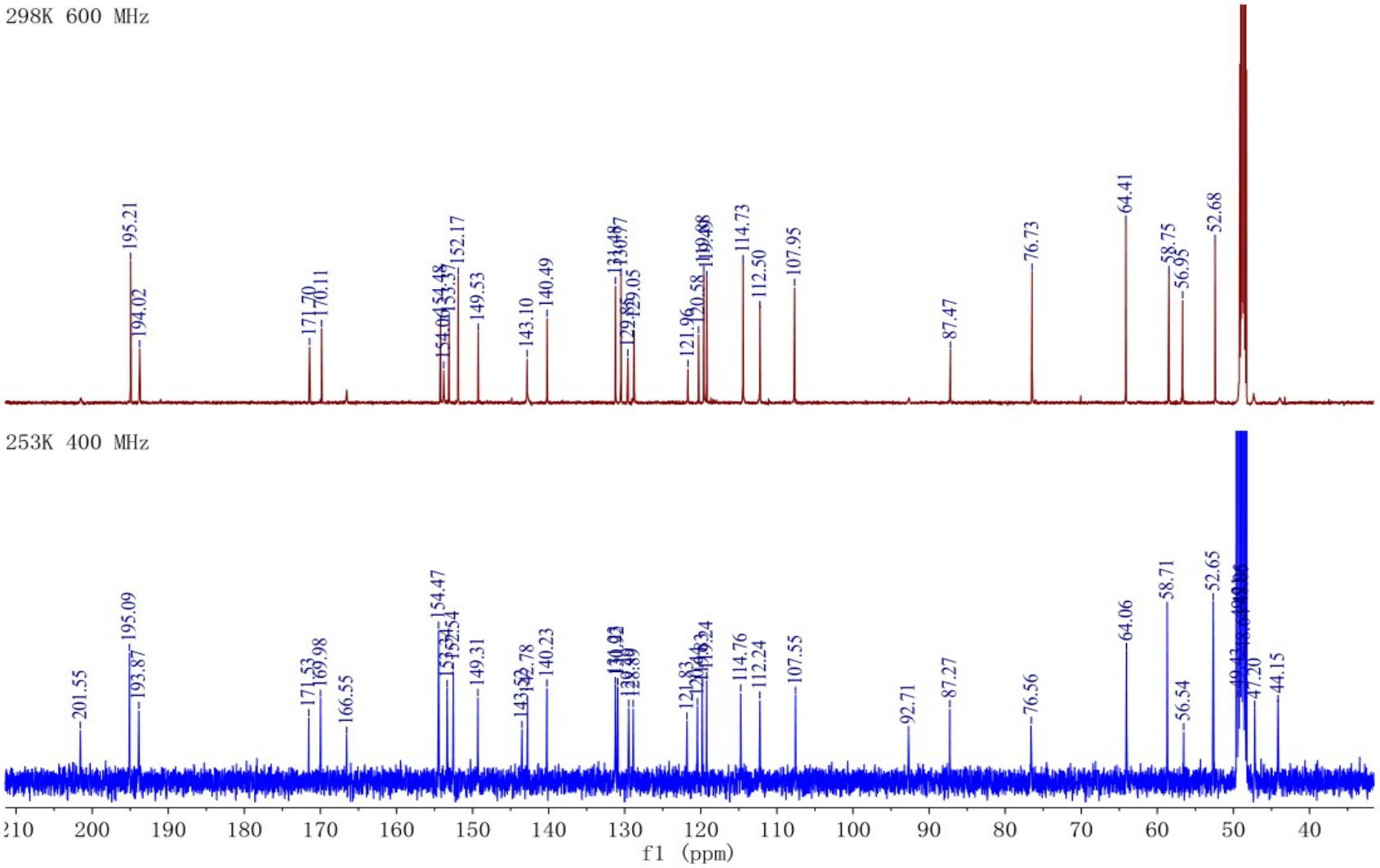

Figure S11. ^{1}H-^{1}H COSY (400 MHz, CD_3OD) spectrum of 1.

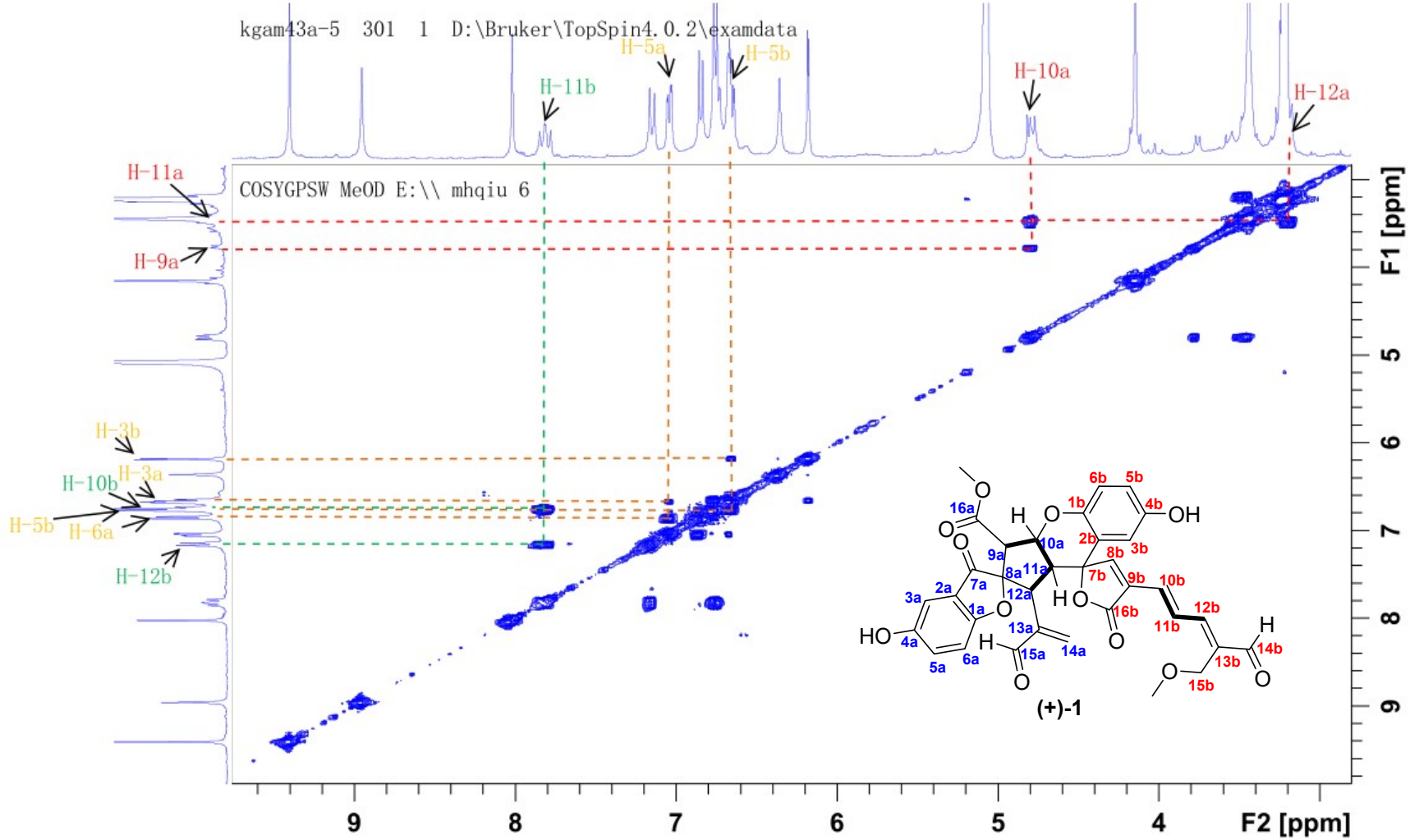

Figure S12. HSQC (400/100 MHz, CD_3OD) spectrum of 1.

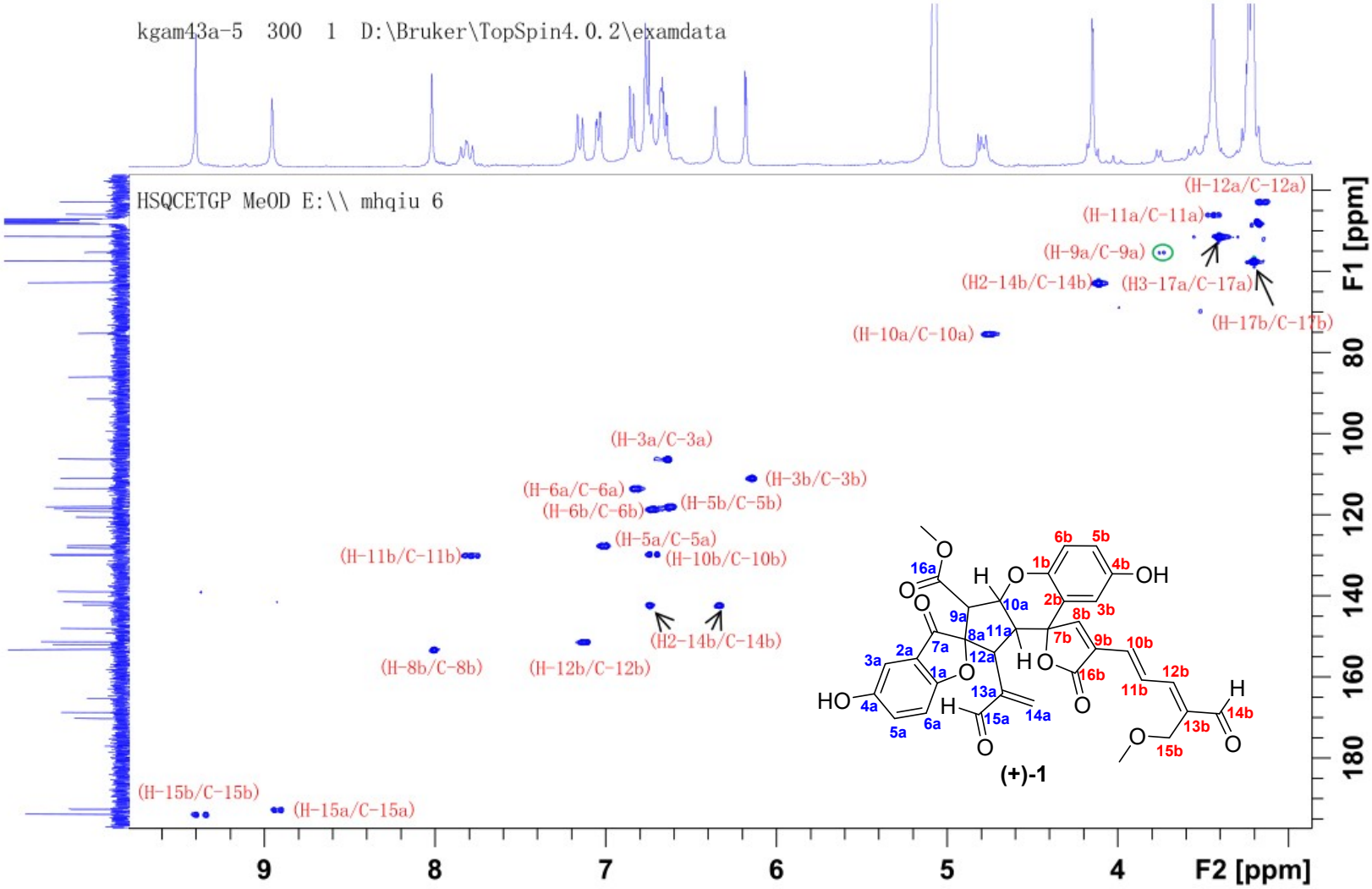

Figure S13. HMBC (400/100 MHz, CD_3OD) spectrum of 1.

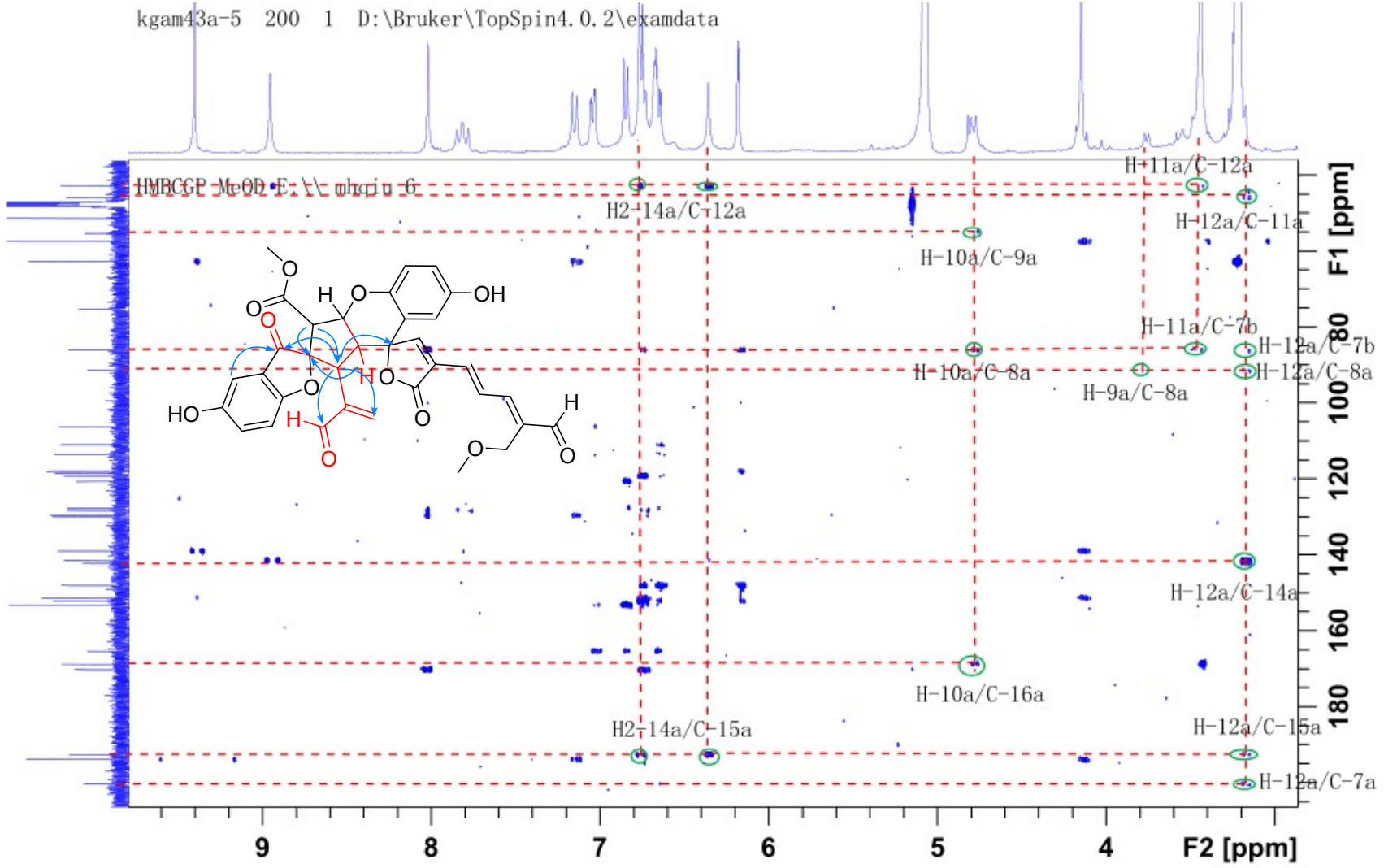

HRESIMS, CD spectra, X-ray crystallographic and computational ECD data of 1

Figure S14. HRESIMS spectrum of 1.

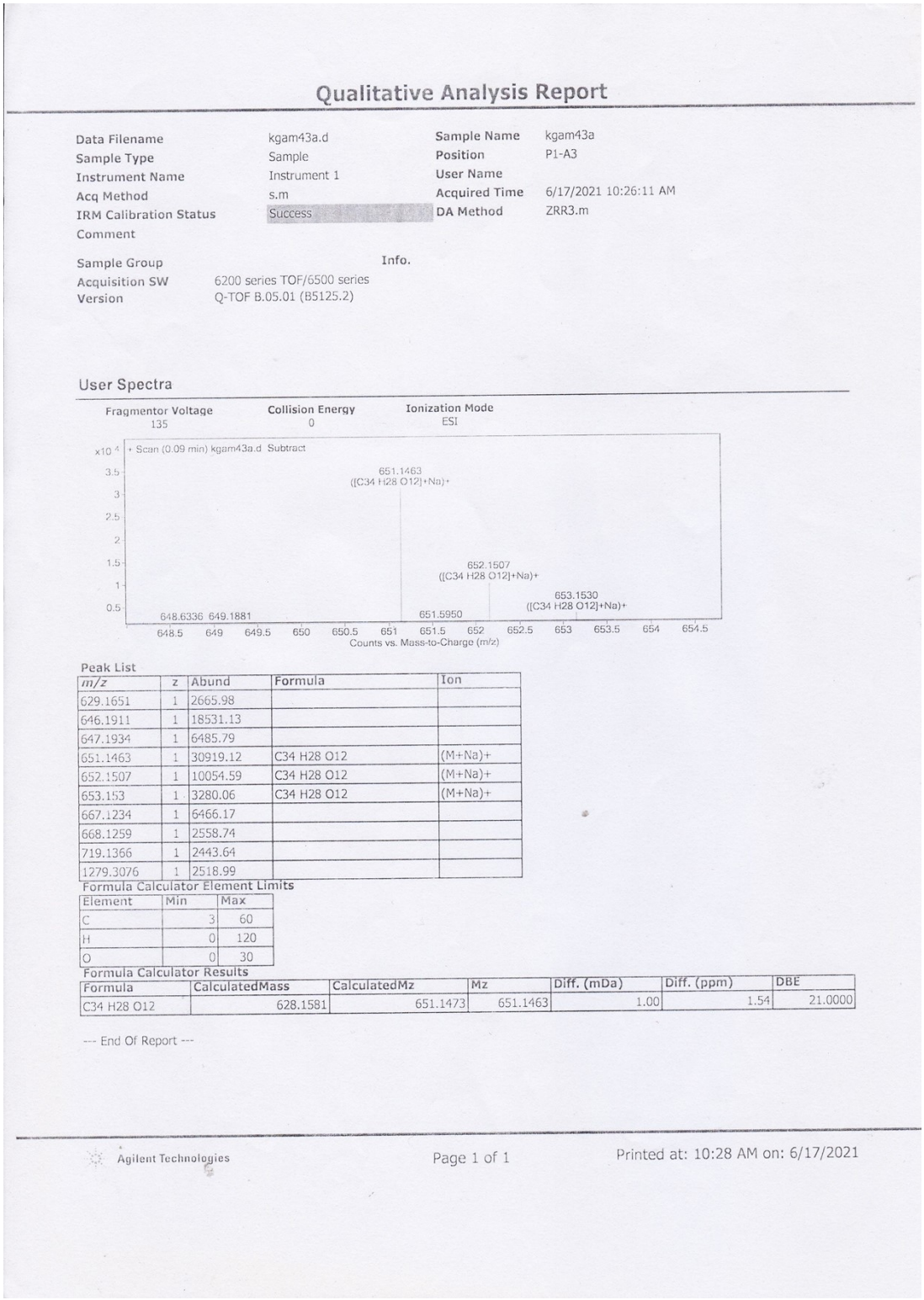

Qualitative Analysis Report

Data Filename	kgam43a.d	Sample Name	kgam43a
Sample Type	Sample	Position	P1-A3
Instrument Name	Instrument 1	User Name	
Acq Method	s.m	Acquired Time	6/17/2021 10:26:11 AM
IRM Calibration Status	Success	DA Method	ZRR3.m
Comment			

Info.

Sample Group	
Acquisition SW Version	6200 series TOF/6500 series Q-TOF B.05.01 (B5125.2)

User Spectra

Fragmentor Voltage	Collision Energy	Ionization Mode
135	0	ESI

Peak List

m/z	z	Abund	Formula	Ion
629.1651	1	2665.98		
646.1911	1	18531.13		
647.1934	1	6485.79		
651.1463	1	30919.12	C34 H28 O12	(M+Na)+
652.1507	1	10054.59	C34 H28 O12	(M+Na)+
653.153	1	3280.06	C34 H28 O12	(M+Na)+
667.1234	1	6466.17		
668.1259	1	2558.74		
719.1366	1	2443.64		
1279.3076	1	2518.99		

Formula Calculator Element Limits

Element	Min	Max
C	3	60
H	0	120
O	0	30

Formula Calculator Results

Formula	CalculatedMass	CalculatedMz	Mz	Diff. (mDa)	Diff. (ppm)	DBE
C34 H28 O12	628.1581	651.1473	651.1463	1.00	1.54	21.0000

--- End Of Report ---

Agilent Technologies Page 1 of 1 Printed at: 10:28 AM on: 6/17/2021

X-ray crystallographic data for 1

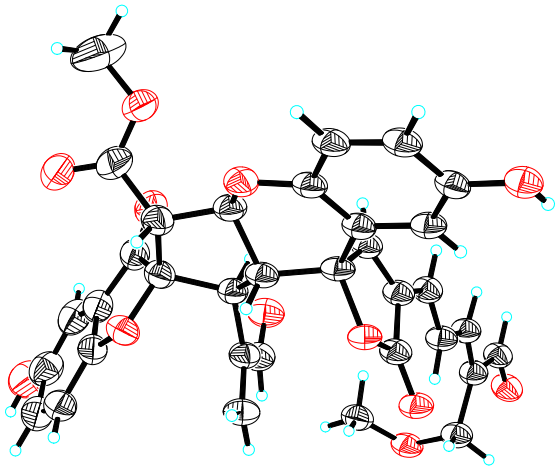

View of a molecule of 1 with the atom-labelling scheme.

Displacement ellipsoids are drawn at the 30% probability level.

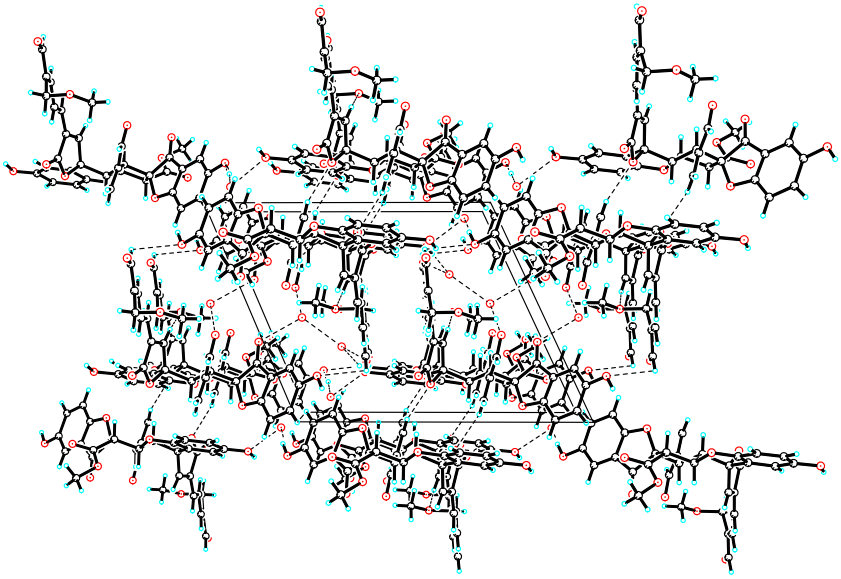

View of the pack drawing of 1.

Hydrogen-bonds are shown as dashed lines.

Table S2. Crystal data and structure refinement for 1.

Identification code	global
Empirical formula	$C_{34}H_{34}O_{15}$
Formula weight	682.61
Temperature	100(2) K
Wavelength	1.54178 Å
Crystal system	Triclinic
Space group	P-1

Unit cell dimensions	a = 9.8432(6) Å, α= 66.313(3)°, b = 12.6520(8) Å, β = 88.319(3)°, c = 14.8226(9) Å, γ = 75.334(3)°
Volume	1629.89(18) Å3
Z	2
Density (calculated)	1.391 mg/m^3
Absorption coefficient	0.937 mm^{-1}
F(000)	716
Crystal size	0.500 × 0.280 × 0.120 mm^3
Theta range for data collection	3.27 to 72.43°
Index ranges	-10<=h<=11, -15<=k<=14, -18<=l<=18
Reflections collected	33527
Independent reflections	6395 [R(int) = 0.0809]
Completeness to theta = 72.43°	98.8 %
Absorption correction	Semi-empirical from equivalents
Max. and min. transmission	0.90 and 0.59
Refinement method	Full-matrix least-squares on F2
Data / restraints / parameters	6395 / 6 / 446
Goodness-of-fit on F2	1.371
Final R indices [I>2sigma(I)]	R1 = 0.1125, wR2 = 0.3355
R indices (all data)	R1 = 0.1407, wR2 = 0.3711
Largest diff. peak and hole	1.011 and -0.590 $e.Å^{-3}$

Figure S15. CD spectrum of (–)-1 and (+)-1.

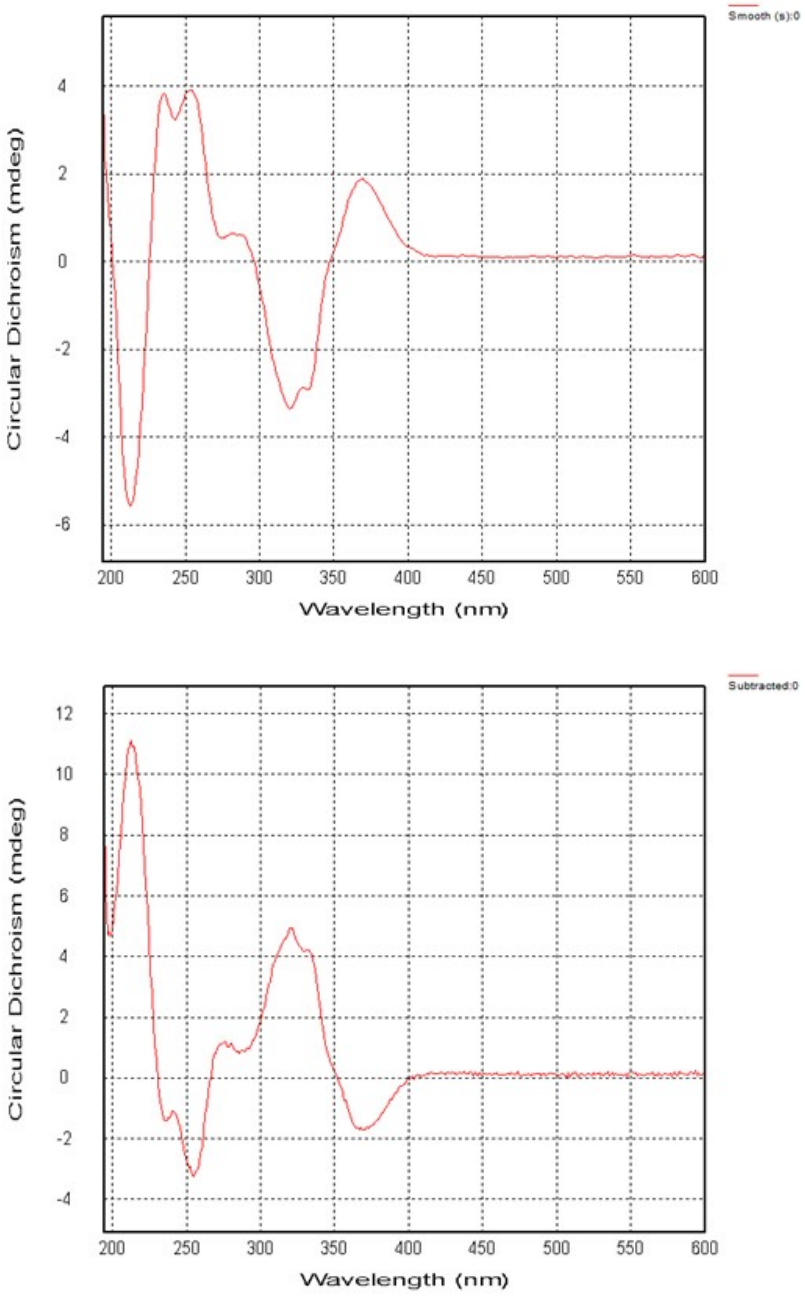

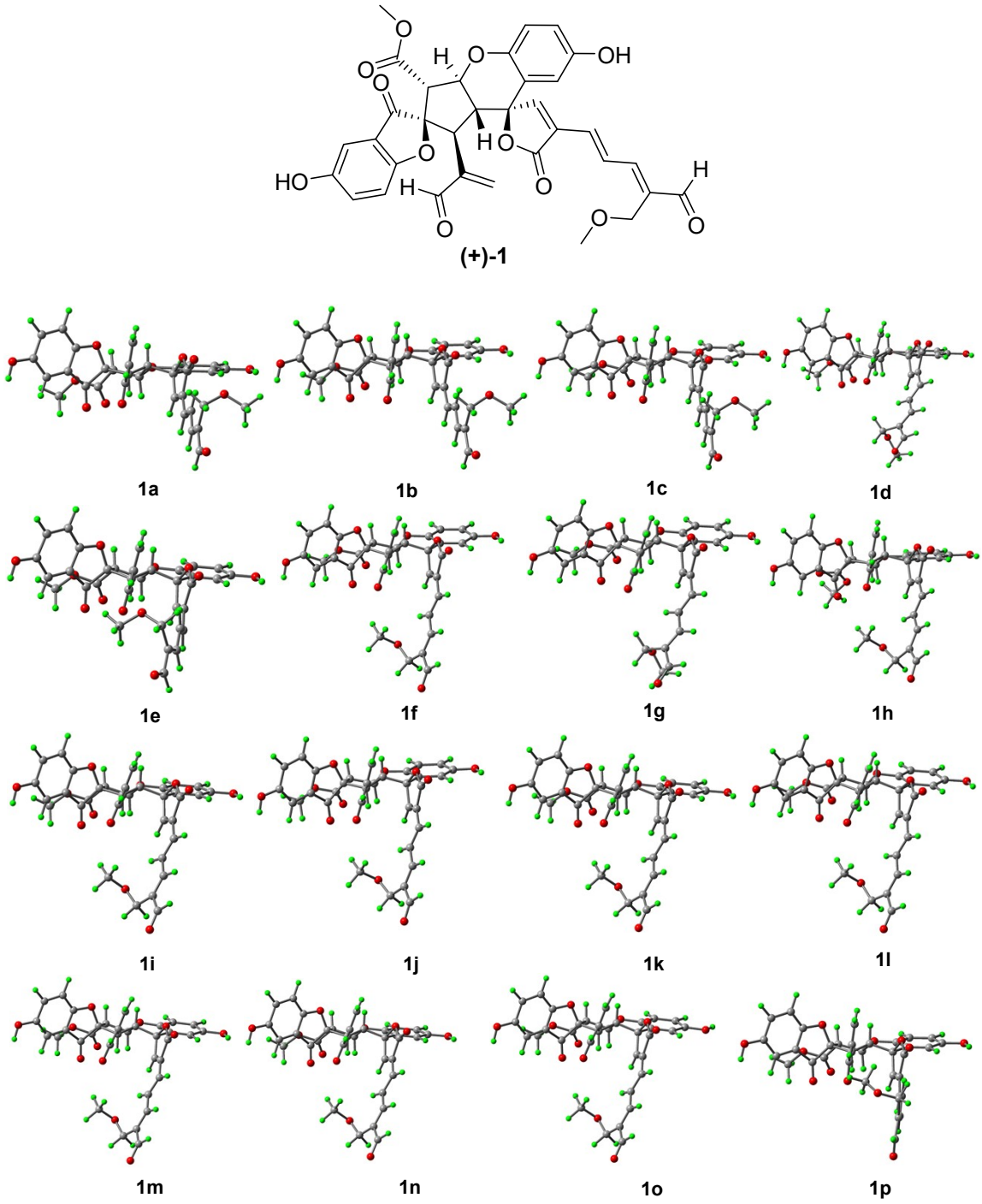

Figure S16. Four optimized conformers of 1a.

Table S3. Conformational analysis of the four optimized conformers of 1a in the gas phase (T = 298.15 K)

Conformer	E (Hartree)	C (Hartree)	G (kcal/mol)	ΔG (kcal/mol)	Population
1a	-2215.140587	0.493936	-1389711.591	0	22.16%
1b	-2215.140588	0.493938	-1389711.591	0.000564759	22.13%
1c	-2215.140588	0.493941	-1389711.589	0.00267319	22.06%

1d	-2215.139069	0.493989	-1389710.606	0.985610189	4.19%
1e	-2215.140357	0.495374	-1389710.544	1.046917858	3.78%
1f	-2215.139017	0.494252	-1389710.407	1.183771383	3.00%
1g	-2215.139107	0.494394	-1389710.375	1.215868488	2.84%
1h	-2215.136746	0.492095	-1389710.336	1.255037626	2.66%
1i	-2215.13903	0.494446	-1389710.294	1.297005454	2.48%
1j	-2215.138996	0.494425	-1389710.286	1.305489381	2.44%
1k	-2215.139004	0.494437	-1389710.283	1.307811166	2.43%
1l	-2215.139	0.494434	-1389710.283	1.30808727	2.43%
1m	-2215.138998	0.494435	-1389710.281	1.310195702	2.42%
1n	-2215.139017	0.494535	-1389710.23	1.361067889	2.22%
1o	-2215.13888	0.494795	-1389709.981	1.610283247	1.46%
1p	-2215.137094	0.493132	-1389709.904	1.687567305	1.28%

Electronic energy obtained at M062X/Def2TZVP SCRF=(IEFPCM, Solvent=Methanol) level of theory; Thermal correction to Gibbs free energy obtained at M062X/def2SVP SCRF=(SMD, Solvent=Methanol), Empirical Dispersion=GD3 level of theory; Gibbs free energy (E + C); The relative Gibbs free energy; The Boltzmann distribution of each conformer.

Table S4. Atomic coordinates (Å) of 1a obtained at the Cam-B3LYP/6-311+G(d,p) level of theory in the MeOH.

C	3.66564	-1.92466	-1.27996	H	3.75617	1.52352	-0.62716
C	3.62777	-2.43337	0.01608	H	1.57731	1.94764	1.45217
C	4.10508	-3.71291	0.32356	H	1.26992	1.54304	-1.56161
C	4.618	-4.47372	-0.72011	H	0.79818	-0.24535	0.88519
C	4.64529	-3.95075	-2.03358	H	0.80645	-0.34893	-2.93329
C	4.17384	-2.68072	-2.33594	H	-0.23668	-1.9014	-2.85947
C	3.04848	-1.3859	0.84889	H	-0.86945	-2.93178	-0.9175
C	2.66867	-0.25957	-0.12607	H	-2.37389	3.85404	-0.60099
C	3.18566	1.16121	0.24142	H	0.06112	7.36974	-0.16764
C	1.93577	2.01465	0.40829	H	2.08456	5.91725	0.1232
C	0.94131	1.3552	-0.52536	H	-0.89724	1.50803	1.82787
C	1.11663	-0.11301	-0.1616	H	-3.03939	-0.10674	2.17967
C	0.38703	-1.12861	-0.99333	H	-4.32621	-0.90777	-0.51219
C	0.3213	-1.12182	-2.332	H	-4.86232	-1.60627	2.49813
C	-0.32917	-2.20546	-0.27067	H	-5.45303	-2.97958	-1.05057
C	4.10842	1.1814	1.43804	H	-7.11441	-3.44854	-0.59943
C	0.9877	4.08581	-0.07689	H	-6.53596	-3.004	3.02978
C	-0.2687	3.4975	-0.28323	H	6.82674	-0.46	2.01186
C	-1.39487	4.31433	-0.43822	H	6.48127	1.19231	2.63598
C	-1.28146	5.70068	-0.39533	H	5.50127	-0.2023	3.203
C	-0.02087	6.28214	-0.19836	H	-8.80804	-1.78383	-0.72904
C	1.09784	5.47997	-0.0372	H	-7.9624	-0.73787	0.45564
C	-0.43766	1.98613	-0.36166	H	-8.30945	-0.12404	-1.18755
C	-1.20795	1.3946	0.78814	H	5.05312	-5.9888	0.37572
C	-2.25182	0.68437	0.32732	H	-3.15742	6.01608	-0.6505
C	-3.18302	-0.12455	1.09475	O	3.92515	1.82511	2.4398
C	-4.16255	-0.88878	0.56685	O	2.84315	-1.34224	2.04176
C	-5.02734	-1.68204	1.41662	O	-0.34813	-2.3074	0.9363
C	-6.01553	-2.48969	0.9661	O	-2.34443	6.52965	-0.53638
C	-6.34829	-2.66089	-0.4982	O	5.10901	-5.72462	-0.55459
C	-6.84852	-3.16294	1.97289	O	3.18167	-0.65927	-1.39202
C	-2.2557	0.83292	-1.15734	O	-1.23376	1.64065	-1.50455
C	6.04482	0.22658	2.35002	O	-6.78749	-1.46717	-1.10901
C	-8.02434	-1.01422	-0.61208	O	2.1453	3.36769	0.08008
H	4.07183	-4.09631	1.34566	O	-7.82157	-3.84107	1.71186
H	5.05589	-4.58475	-2.82187	O	-2.99133	0.35772	-1.98023
H	4.20161	-2.28657	-3.35186	O	5.15641	0.39221	1.24396

Table S5. Atomic coordinates (Å) of 1b obtained at the Cam-B3LYP/6-311+G(d,p) level of theory in the MeOH.

C	3.66517	-1.92496	-1.28005	H	3.75628	1.5231	-0.62715
C	3.62733	-2.43368	0.01599	H	1.57747	1.9477	1.4521
C	4.10447	-3.71329	0.32344	H	1.2699	1.543	-1.56166
C	4.61724	-4.47414	-0.72027	H	0.79802	-0.24523	0.88524
C	4.64454	-3.95116	-2.03372	H	0.80567	-0.34864	-2.93318
C	4.17322	-2.68109	-2.33606	H	-0.23746	-1.90111	-2.85929
C	3.04816	-1.38618	0.84882	H	-0.86993	-2.9316	-0.91726
C	2.66844	-0.25978	-0.12608	H	-2.37349	3.85463	-0.60089
C	3.18568	1.16091	0.24142	H	0.06211	7.36991	-0.16758
C	1.93592	2.01457	0.40822	H	2.08533	5.91711	0.12309
C	0.94134	1.35523	-0.52538	H	-0.89715	1.50849	1.82792
C	1.11645	-0.11298	-0.16157	H	-3.03939	-0.1062	2.17979
C	0.38666	-1.12851	-0.99321	H	-4.32613	-0.90733	-0.51207
C	0.32066	-1.1216	-2.33186	H	-4.86232	-1.6058	2.49822
C	-0.32946	-2.20538	-0.27049	H	-5.45258	-2.97946	-1.05042
C	4.1084	1.18098	1.43806	H	-7.11397	-3.44847	-0.59941
C	0.98817	4.08585	-0.077	H	-6.53585	-3.00371	3.02982
C	-0.26833	3.49773	-0.28329	H	6.48062	1.19186	2.63651
C	-1.39437	4.31473	-0.4382	H	5.50134	-0.20354	3.2028
C	-1.28075	5.70107	-0.39527	H	6.82704	-0.45997	2.01165
C	-0.02007	6.28233	-0.19835	H	-8.80761	-1.784	-0.72908
C	1.09854	5.47999	-0.03729	H	-7.96217	-0.73758	0.45534
C	-0.43754	1.98639	-0.36163	H	-8.30928	-0.12427	-1.18804
C	-1.20786	1.39497	0.78819	H	5.05242	-5.98925	0.37552
C	-2.25182	0.68484	0.32741	H	-3.15678	6.01682	-0.64973
C	-3.18302	-0.12404	1.09487	O	3.92512	1.82466	2.43985
C	-4.1625	-0.88832	0.56697	O	2.84288	-1.3425	2.04171
C	-5.02725	-1.68165	1.41671	O	-0.34823	-2.30739	0.93648
C	-6.01528	-2.48947	0.96615	O	-2.34358	6.53022	-0.53627
C	-6.3479	-2.66078	-0.49816	O	5.10814	-5.72511	-0.55481
C	-6.84825	-3.16282	1.97291	O	3.18136	-0.65952	-1.39209
C	-2.25568	0.83331	-1.15726	O	-1.23372	1.64099	-1.50451
C	6.04473	0.22603	2.35006	O	-6.78711	-1.46711	-1.10908
C	-8.02404	-1.01423	-0.61231	O	2.14567	3.36755	0.07991
H	4.07125	-4.09665	1.34555	O	-7.82116	-3.84113	1.71183
H	5.05503	-4.5852	-2.82204	O	-2.99133	0.35806	-1.98011
H	4.201	-2.28693	-3.35197	O	5.1563	0.39168	1.24402

Table S6. Atomic coordinates (Å) of 1c obtained at the Cam-B3LYP/6-311+G(d,p) level of theory in the MeOH.

C	3.66516	-1.92511	-1.27995	H	3.75616	1.52307	-0.62746
C	3.62728	-2.43369	0.01615	H	1.57751	1.94766	1.45198
C	4.10438	-3.71328	0.32375	H	1.26981	1.54306	-1.56177
C	4.61717	-4.47426	-0.71985	H	0.79797	-0.24528	0.88507
C	4.64449	-3.95143	-2.03337	H	0.80574	-0.34851	-2.93335
C	4.17321	-2.68138	-2.33586	H	-0.2374	-1.90098	-2.85957
C	3.0481	-1.38609	0.84885	H	-0.86988	-2.9316	-0.91757
C	2.66843	-0.25979	-0.12619	H	-2.37355	3.85465	-0.60058
C	3.18568	1.1609	0.2412	H	0.06209	7.36992	-0.16733
C	1.93593	2.01455	0.40808	H	2.08534	5.9171	0.12306
C	0.94131	1.35524	-0.52549	H	-0.89709	1.50837	1.8279
C	1.11644	-0.11298	-0.16173	H	-3.03914	-0.10656	2.17975
C	0.38667	-1.12848	-0.99343	H	-4.32625	-0.90717	-0.5121
C	0.32069	-1.12149	-2.33208	H	-4.86212	-1.60613	2.49815
C	-0.32945	-2.20538	-0.27075	H	-5.45278	-2.97926	-1.05064
C	4.10853	1.18108	1.43773	H	-7.11416	-3.44827	-0.59953
C	0.98816	4.08586	-0.077	H	-6.53557	-3.00414	3.0297
C	-0.26835	3.49774	-0.28321	H	6.82731	-0.45971	2.01114
C	-1.39441	4.31475	-0.43798	H	6.48079	1.19212	2.63596
C	-1.28079	5.70108	-0.39497	H	5.50172	-0.20336	3.20244
C	-0.02009	6.28234	-0.19815	H	-8.30934	-0.12388	-1.18749
C	1.09854	5.47999	-0.03725	H	-8.80777	-1.78371	-0.72895
C	-0.43757	1.98641	-0.36163	H	-7.96221	-0.73766	0.45571
C	-1.20784	1.3949	0.78818	H	5.0523	-5.98928	0.3761
C	-2.25179	0.68477	0.32739	H	-3.15686	6.01683	-0.64908
C	-3.18291	-0.12421	1.09484	O	3.92537	1.82488	2.43946
C	-4.16249	-0.88837	0.56693	O	2.84281	-1.34227	2.04173
C	-5.02717	-1.68182	1.41664	O	-0.34826	-2.3074	0.93621
C	-6.01525	-2.48955	0.96606	O	-2.34364	6.53023	-0.53577
C	-6.34804	-2.66062	-0.49825	O	5.10805	-5.72521	-0.55425
C	-6.84811	-3.16306	1.9728	O	3.1814	-0.65967	-1.39215
C	-2.25574	0.83336	-1.15726	O	-1.2338	1.64108	-1.5045
C	6.04497	0.22623	2.34962	O	-6.78725	-1.46685	-1.10894
C	-8.02414	-1.01402	-0.612	O	2.14568	3.36753	0.07979
H	4.07113	-4.0965	1.34592	O	-7.82104	-3.84133	1.71172
H	5.05499	-4.58557	-2.8216	O	-2.99143	0.35817	-1.98011
H	4.20103	-2.28734	-3.35182	O	5.15639	0.39173	1.24367

Table S7. Atomic coordinates (Å) of 1d obtained at the Cam-B3LYP/6-311+G(d,p) level of theory in the MeOH.

C	3.75825	0.89705	-1.17925	H	1.70565	3.33586	0.32886
C	3.85995	-0.03235	-0.14684	H	-0.52166	1.69257	1.59883
C	4.94389	-0.91225	-0.04705	H	-0.15691	2.49499	-1.32763
C	5.9253	-0.8341	-1.02753	H	0.2127	-0.10876	0.25372
C	5.81087	0.10952	-2.07413	H	0.50711	1.32192	-3.25692
C	4.73622	0.983	-2.16978	H	0.75794	-0.41273	-3.91259
C	2.68389	0.16096	0.69404	H	0.91814	-2.28236	-2.58206
C	1.84242	1.22423	-0.03137	H	-4.57395	1.96968	-0.98585
C	1.36783	2.42109	0.83935	H	-4.78987	5.63985	1.24029
C	-0.15228	2.36445	0.8015	H	-2.33647	5.46852	1.73625
C	-0.43929	1.75695	-0.55826	H	-2.23755	-0.12557	0.89019
C	0.52285	0.57516	-0.55305	H	-3.50779	-2.49783	-2.05137
C	0.66297	-0.23639	-1.80851	H	-1.69887	-2.61124	0.45255
C	0.64326	0.25646	-3.05458	H	-3.27946	-4.77193	-1.18212
C	0.84546	-1.69651	-1.63986	H	-0.44306	-5.87605	1.78704
C	1.95112	2.43183	2.23302	H	-0.12891	-4.32593	0.95742
C	-2.09071	3.63556	0.65139	H	-3.02621	-6.94633	-0.64499
C	-2.71484	2.64328	-0.1179	H	3.70429	3.17373	4.09039
C	-4.08638	2.74067	-0.38195	H	3.66903	1.38396	3.94136
C	-4.83184	3.81182	0.10142	H	5.02394	2.32019	3.21338
C	-4.19884	4.80288	0.86509	H	-3.27861	-5.24287	2.6373
C	-2.84371	4.70905	1.13929	H	-1.92926	-5.85691	3.64477
C	-1.93413	1.47858	-0.71267	H	-2.72626	-4.30482	4.056
C	-2.30464	0.12092	-0.17069	H	7.00556	-2.23267	-0.28298
C	-2.63641	-0.69404	-1.18443	H	-6.47745	3.21724	-0.68371
C	-2.89535	-2.1272	-1.22313	O	1.30606	2.44013	3.2504
C	-2.34904	-2.98887	-0.34261	O	2.34979	-0.37419	1.72755
C	-2.56193	-4.42014	-0.43132	O	0.91311	-2.23917	-0.55756
C	-1.92469	-5.32982	0.34125	O	-6.15946	3.94818	-0.13412
C	-0.91314	-4.95545	1.40122	O	7.01829	-1.63296	-1.04377
C	-2.29386	-6.74305	0.16876	O	2.65047	1.68262	-1.1102
C	-2.61275	0.1193	-2.42939	O	-2.23809	1.37316	-2.11393
C	3.95465	2.32166	3.44521	O	-1.47282	-4.20909	2.45987
C	-2.39423	-4.94537	3.22875	O	-0.75348	3.62716	0.95333
H	5.00873	-1.63401	0.77013	O	-1.86115	-7.64852	0.85183
H	6.60591	0.13448	-2.822	O	-2.86077	-0.21556	-3.55653
H	4.65784	1.70776	-2.98029	O	3.27683	2.43275	2.19289

Table S8. Atomic coordinates (Å) of 1e obtained at the Cam-B3LYP/6-311+G(d,p) level of theory in the MeOH.

C	0.3258	-3.57815	-1.29983	H	3.32561	-1.90393	-0.49456
C	-0.2204	-3.76741	-0.03276	H	2.46913	0.21406	1.51194
C	-1.13839	-4.79015	0.23254	H	2.14384	0.24871	-1.52637
C	-1.50056	-5.61674	-0.8241	H	0.18396	-0.23779	0.78406
C	-0.9425	-5.41464	-2.10745	H	0.44121	-0.36996	-3.02687
C	-0.02946	-4.40182	-2.36759	H	-1.42564	-0.2774	-3.1229
C	0.36606	-2.74166	0.82229	H	-2.80661	-0.22847	-1.31948
C	1.21369	-1.87105	-0.11977	H	2.22369	4.55325	-0.66057
C	2.67299	-1.58678	0.33303	H	6.4657	4.24151	-0.03731
C	2.76451	-0.07454	0.48631	H	6.21908	1.77212	0.32101
C	1.74779	0.43687	-0.51395	H	0.89248	2.11078	1.81307
C	0.55039	-0.46139	-0.23094	H	-1.641	3.25031	2.06671
C	-0.61712	-0.3754	-1.17369	H	-3.0637	2.69787	-0.6186
C	-0.52127	-0.34179	-2.51033	H	-4.05546	3.48732	2.24897
C	-1.97511	-0.31229	-0.58573	H	-6.73852	1.93441	-0.66265
C	3.08655	-2.35928	1.56408	H	-5.29344	2.7296	-1.34284
C	4.09514	1.78641	0.02792	H	-6.24488	3.32169	2.73756
C	2.96392	2.56785	-0.25194	H	2.97	-5.52475	2.18112
C	3.10737	3.94672	-0.44196	H	4.20224	-4.39921	2.85474
C	4.35935	4.54991	-0.36582	H	2.47787	-4.22647	3.3276
C	5.48711	3.76236	-0.09466	H	-4.89766	-1.08004	-0.04802
C	5.35145	2.39705	0.10368	H	-5.19021	0.10518	1.25757
C	1.58064	1.94627	-0.36257	H	-6.50782	-0.30713	0.11203
C	0.65002	2.30033	0.76648	H	-2.71392	-6.6842	0.21135
C	-0.50984	2.76246	0.27327	H	3.69633	6.31583	-0.71423
C	-1.74009	3.04786	0.99585	O	3.50344	-1.86575	2.58105
C	-2.96435	2.95344	0.43926	O	0.23391	-2.52531	2.00661
C	-4.16948	3.09474	1.23147	O	-2.19555	-0.33526	0.60613
C	-5.40039	2.72479	0.80895	O	4.5445	5.88069	-0.5437
C	-5.65241	2.07859	-0.5332	O	-2.38562	-6.63356	-0.6987
C	-6.50818	2.8426	1.7676	O	1.20907	-2.547	-1.3724
C	-0.35223	2.84017	-1.20871	O	0.89775	2.44294	-1.52247
C	3.16364	-4.50073	2.51428	O	-4.97343	0.84877	-0.68212
C	-5.41878	-0.14807	0.2074	O	4.05328	0.42895	0.22099
H	-1.5578	-4.92561	1.23183	O	-7.6378	2.44945	1.55843
H	-1.25678	-6.08774	-2.90748	O	-1.13737	3.18752	-2.04907
H	0.39393	-4.25425	-3.3612	O	2.92948	-3.66332	1.38113

Table S9. Atomic coordinates (Å) of 1f obtained at the Cam-B3LYP/6-311+G(d,p) level of theory in the MeOH.

C	3.75666	-0.97162	1.1467	H	1.60098	-3.32981	-0.39211
C	3.82304	0.01152	0.16203	H	-0.56291	-1.55528	-1.59217
C	4.89956	0.90154	0.07554	H	-0.26061	-2.54738	1.28404
C	5.91106	0.7777	1.02005	H	0.20709	0.15749	-0.0878
C	5.83321	-0.22086	2.01795	H	0.4273	-1.59407	3.27535
C	4.76559	-1.10441	2.1003	H	0.76848	0.0593	4.08264
C	2.61976	-0.14002	-0.64739	H	1.04251	2.02354	2.93297
C	1.80279	-1.24069	0.0505	H	-4.62315	-1.88861	1.02453
C	1.29461	-2.38529	-0.86765	H	-4.93613	-5.45236	-1.35837
C	-0.22278	-2.28349	-0.83236	H	-2.4906	-5.29437	-1.89338
C	-0.49862	-1.74983	0.56037	H	-2.21072	0.17609	-0.92182
C	0.50454	-0.60776	0.64723	H	-3.20283	2.66418	2.07188
C	0.68021	0.07676	1.97235	H	-2.0359	2.59899	-0.79376
C	0.6235	-0.52429	3.1685	H	-3.10564	4.849	1.09516
C	0.94469	1.53235	1.94029	H	-2.59394	5.04371	-2.89504
C	1.8842	-2.35765	-2.25799	H	-1.18369	6.01439	-2.44184
C	-2.19603	-3.51546	-0.73337	H	-3.17008	6.94214	0.51349
C	-2.79206	-2.55027	0.09166	H	3.64454	-3.05361	-4.12467
C	-4.15914	-2.63955	0.37845	H	3.61216	-1.26787	-3.93278
C	-4.92932	-3.67779	-0.13741	H	4.96178	-2.22408	-3.22125
C	-4.3259	-4.64142	-0.95764	H	0.77266	3.09448	-1.79153
C	-2.97456	-4.5548	-1.25362	H	0.85384	4.86619	-2.05886
C	-1.98237	-1.41524	0.70209	H	0.14016	4.21446	-0.54912
C	-2.29416	-0.05207	0.14194	H	6.95595	2.22562	0.32247
C	-2.58864	0.79319	1.14293	H	-6.54935	-3.09339	0.70469
C	-2.79661	2.23417	1.151	O	1.24331	-2.33735	-3.27782
C	-2.46703	3.02951	0.11273	O	2.24992	0.44725	-1.64052
C	-2.66602	4.4648	0.16664	O	1.05173	2.16742	0.91333
C	-2.37001	5.37257	-0.79357	O	-6.25394	-3.80559	0.11904
C	-1.77574	5.12471	-2.16077	O	6.99982	1.5818	1.04512
C	-2.71822	6.77096	-0.48941	O	2.64916	-1.75731	1.07098
C	-2.60212	-0.00571	2.39783	O	-2.29872	-1.28415	2.0965
C	3.89362	-2.21783	-3.4581	O	-1.00092	3.96086	-2.28171
C	0.2484	4.04616	-1.6341	O	-0.86371	-3.51585	-1.05863
H	4.9357	1.66634	-0.70339	O	-2.54694	7.69423	-1.25892
H	6.65085	-0.28033	2.739	O	-2.82954	0.35371	3.52153
H	4.7151	-1.87102	2.87368	O	3.20978	-2.35792	-2.21193

Table S10. Atomic coordinates (Å) of 1g obtained at the Cam-B3LYP/6-311+G(d,p) level of theory in the MeOH.

C	3.63054	1.27274	-1.18636	H	1.31296	3.5159	0.27001
C	3.81962	0.37351	-0.13948	H	-0.69977	1.64441	1.58522
C	4.98229	-0.39771	-0.02653	H	-0.44952	2.46111	-1.3493
C	5.9527	-0.24066	-1.00856	H	0.21236	-0.07672	0.24354
C	5.75061	0.67259	-2.06862	H	0.29152	1.35158	-3.27493
C	4.59741	1.43753	-2.17768	H	0.75655	-0.34144	-3.92201
C	2.62805	0.4645	0.69702	H	1.18686	-2.15903	-2.58302
C	1.68766	1.42641	-0.04809	H	-4.77747	1.43492	-0.95823
C	1.08754	2.57934	0.80283	H	-5.39723	5.06773	1.25422
C	-0.41626	2.34932	0.78095	H	-2.9357	5.18615	1.72341
C	-0.64299	1.70269	-0.5722	H	-2.20094	-0.36499	0.89685
C	0.44457	0.63535	-0.5652	H	-3.20878	-2.8794	-2.02965
C	0.6717	-0.15985	-1.81808	H	-1.38738	-2.77154	0.46532
C	0.56917	0.31513	-3.06705	H	-2.71273	-5.1084	-1.15355
C	1.04313	-1.58244	-1.64343	H	0.27134	-5.85932	1.78044
C	1.67673	2.68857	2.1894	H	0.37767	-4.27894	0.95512
C	-2.48926	3.38821	0.64387	H	-2.19914	-7.23481	-0.61555
C	-3.00199	2.32606	-0.11395	H	3.36582	3.65841	4.00317
C	-4.37802	2.26131	-0.36301	H	3.49406	1.86889	3.91688
C	-5.23826	3.24069	0.12387	H	4.75257	2.89857	3.14374
C	-4.71692	4.30302	0.87611	H	-1.17361	-6.03009	3.66263
C	-3.35715	4.36928	1.13562	H	-2.15492	-4.59239	4.09071
C	-2.09809	1.25699	-0.71293	H	-2.6057	-5.59162	2.67817
C	-2.30554	-0.13165	-0.16395	H	7.15536	-1.52432	-0.2488
C	-2.54954	-0.98332	-1.1724	H	-6.81206	2.44864	-0.63393
C	-2.64009	-2.43697	-1.20552	O	1.04045	2.66677	3.2121
C	-1.9922	-3.22557	-0.32563	O	2.34636	-0.08194	1.74016
C	-2.03489	-4.67225	-0.41008	O	1.1853	-2.10527	-0.55854
C	-1.28709	-5.49769	0.35785	O	-6.57497	3.22005	-0.09887
C	-0.31546	-5.00338	1.40574	O	7.11618	-0.93252	-1.01449
C	-1.48895	-6.94495	0.19137	O	2.45179	1.9489	-1.12946
C	-2.63072	-0.17754	-2.41981	O	-2.39975	1.11244	-2.11117
C	3.68915	2.81044	3.38556	O	-0.94888	-4.33645	2.47584
C	-1.75708	-5.18471	3.25663	O	-1.15665	3.5361	0.93013
H	5.11461	-1.09808	0.80095	O	-0.947	-7.79175	0.87178
H	6.5407	0.76208	-2.81671	O	-2.84764	-0.54316	-3.54372
H	4.4515	2.13949	-2.99873	O	2.99593	2.81474	2.13677

Table S11. Atomic coordinates (Å) of 1h obtained at the Cam-B3LYP/6-311+G(d,p) level of theory in the MeOH.

C	-3.69811	-1.44666	-1.09884	H	-1.10682	-3.53879	0.17762
C	-3.83916	-0.51177	-0.07611	H	0.72924	-1.49199	1.48965
C	-5.01482	0.22864	0.09266	H	0.56459	-2.44322	-1.41044
C	-6.04948	0.00239	-0.80686	H	-0.30563	0.12799	0.01539
C	-5.89528	-0.94576	-1.84408	H	-0.4822	-1.66324	-3.34058
C	-4.72853	-1.67948	-2.00928	H	-0.99262	-0.04931	-4.13892
C	-2.58448	-0.52672	0.66792	H	-1.36877	1.89523	-2.98351
C	-1.67303	-1.49711	-0.10316	H	4.76103	-1.09575	-1.17309
C	-0.97809	-2.59646	0.73532	H	5.67322	-4.62742	1.10092
C	0.50457	-2.24478	0.71129	H	3.24087	-4.88117	1.65833
C	0.67557	-1.63578	-0.66734	H	2.08267	0.49453	0.86037
C	-0.49821	-0.66806	-0.721	H	2.66478	3.19478	-2.05767
C	-0.79928	-0.0065	-2.03487	H	1.55785	2.8722	0.81426
C	-0.75534	-0.6107	-3.23011	H	2.27298	5.31222	-1.00514
C	-1.17257	1.42527	-1.99502	H	1.76724	5.28142	2.98898
C	-1.61248	-2.82319	2.08703	H	0.23641	6.07235	2.57949
C	2.64975	-3.14017	0.55554	H	2.0386	7.37324	-0.35037
C	3.07259	-2.0694	-0.24546	H	-1.86827	-4.21885	4.32144
C	4.43225	-1.92957	-0.54598	H	-0.35759	-3.49282	4.97872
C	5.3664	-2.84287	-0.06589	H	-1.81053	-2.46561	4.70218
C	4.93569	-3.91456	0.72881	H	-1.3132	2.94201	1.80841
C	3.59166	-4.05535	1.03739	H	-1.63315	4.67409	2.14775
C	2.08305	-1.06162	-0.81244	H	-0.84334	4.18673	0.6137
C	2.1856	0.31546	-0.21115	H	-7.23926	1.27518	-0.00608
C	2.33981	1.2266	-1.18559	H	6.86594	-1.97684	-0.89404
C	2.3384	2.68195	-1.14737	O	-2.80637	-2.82295	2.26735
C	1.91265	3.38855	-0.08047	O	-2.23291	0.09919	1.64324
C	1.90124	4.8383	-0.08836	O	-1.25893	2.06524	-0.96925
C	1.48354	5.66081	0.90295	O	6.69178	-2.74702	-0.33339
C	0.93953	5.28167	2.26094	O	-7.23333	0.65708	-0.75182
C	1.62149	7.1044	0.64613	O	-2.49669	-2.08327	-1.10462
C	2.45389	0.47891	-2.46686	O	2.35163	-0.83978	-2.2054
C	-1.23089	-3.32529	4.3416	O	0.3283	4.02055	2.33635
C	-0.92375	3.96182	1.69076	O	1.33964	-3.36294	0.89386
H	-5.10937	0.95794	0.90025	O	1.32243	7.96668	1.44674
H	-6.73433	-1.08855	-2.52784	O	2.60537	0.90448	-3.58013
H	-4.61948	-2.40858	-2.81233	O	-0.72043	-3.05671	3.03332

Table S12. Atomic coordinates (Å) of 1i obtained at the Cam-B3LYP/6-311+G(d,p) level of theory in the MeOH.

C	3.7628	0.95313	-1.14579	H	1.61759	3.3226	0.39082
C	3.82406	-0.02986	-0.16064	H	-0.55482	1.55883	1.59153
C	4.89578	-0.92557	-0.0738	H	-0.24678	2.54787	-1.28508
C	5.90789	-0.80763	-1.01843	H	0.20767	-0.15838	0.08849
C	5.83552	0.19116	-2.01651	H	0.43664	1.58946	-3.27603
C	4.77257	1.08032	-2.09925	H	0.77075	-0.06605	-4.08183
C	2.6215	0.1282	0.64861	H	1.03575	-2.03049	-2.93066
C	1.80996	1.23225	-0.05019	H	-4.61298	1.90839	-1.02512
C	1.30682	2.37985	0.86701	H	-4.91053	5.47391	1.35717
C	-0.211	2.28499	0.83142	H	-2.4654	5.3063	1.89104
C	-0.48886	1.75183	-0.56111	H	-2.21093	-0.16625	0.91992
C	0.50898	0.60498	-0.64699	H	-3.21245	-2.64901	-2.07542
C	0.6819	-0.0814	-1.97155	H	-2.05185	-2.58889	0.79284
C	0.62812	0.51892	-3.16822	H	-3.12845	-4.8345	-1.09743
C	0.94038	-1.53808	-1.93834	H	-2.62587	-5.03328	2.8946
C	1.89605	2.35054	2.25747	H	-1.21734	-6.00694	2.44263
C	-2.17859	3.5258	0.73151	H	-3.20554	-6.92693	-0.51425
C	-2.77887	2.5629	-0.09309	H	3.61896	1.25391	3.93322
C	-4.14571	2.65762	-0.37939	H	4.97281	2.20391	3.22144
C	-4.9115	3.69895	0.13679	H	3.65889	3.0396	4.12406
C	-4.30372	4.66046	0.95631	H	0.11376	-4.21016	0.55388
C	-2.95262	4.56853	1.25168	H	0.74674	-3.09083	1.79671
C	-1.97413	1.42431	-0.70345	H	0.82416	-4.86259	2.06482
C	-2.2927	0.06251	-0.14385	H	6.94339	-2.26289	-0.32209
C	-2.59082	-0.78105	-1.14521	H	-6.53538	3.11978	-0.70195
C	-2.80601	-2.22096	-1.15373	O	1.25493	2.33393	3.27721
C	-2.4828	-3.01768	-0.11454	O	2.24872	-0.45658	1.64211
C	-2.68893	-4.45197	-0.16816	O	1.04544	-2.17277	-0.91093
C	-2.39961	-5.36068	0.79321	O	-6.23583	3.83202	-0.11848
C	-1.80675	-5.1155	2.16149	O	6.99197	-1.61801	-1.0435
C	-2.7546	-6.75741	0.48934	O	2.65914	1.74431	-1.07068
C	-2.59965	0.01822	-2.39991	O	-2.29043	1.29512	-2.09808
C	3.90458	2.20237	3.45804	O	-1.02923	-3.95372	2.28474
C	0.22086	-4.04158	1.63893	O	-0.84626	3.52048	1.05666
H	4.92778	-1.69036	0.70533	O	-2.58967	-7.68094	1.25991
H	6.65347	0.24604	-2.73757	O	-2.82813	-0.33981	-3.52385
H	4.72622	1.8469	-2.87293	O	3.22164	2.34462	2.21163

Table S13. Atomic coordinates (Å) of 1j obtained at the Cam-B3LYP/6-311+G(d,p) level of theory in the MeOH.

C	-3.7486	-0.99635	-1.14777	H	-1.58164	-3.33674	0.39942
C	-3.82241	-0.01147	-0.16535	H	0.57396	-1.54903	1.59419
C	-4.9058	0.87048	-0.0809	H	0.27664	-2.54708	-1.2805
C	-5.91634	0.73646	-1.02501	H	-0.20601	0.15722	0.08737
C	-5.83042	-0.26316	-2.02118	H	-0.41852	-1.60152	-3.2728
C	-4.75606	-1.13861	-2.10155	H	-0.76712	0.04882	-4.08308
C	-2.61852	-0.1528	0.64497	H	-1.04929	2.01409	-2.93666
C	-1.79384	-1.24994	-0.04949	H	4.6345	-1.8675	-1.02515
C	-1.27953	-2.3893	0.87184	H	4.96526	-5.42838	1.35955
C	0.23737	-2.28011	0.83559	H	2.51996	-5.2796	1.89819
C	0.51027	-1.74719	-0.55798	H	2.21144	0.18765	0.92453
C	-0.49899	-0.61073	-0.64657	H	3.19405	2.68104	-2.06714
C	-0.6781	0.0706	-1.97282	H	2.01501	2.61128	0.79355
C	-0.61929	-0.5324	-3.16789	H	3.07986	4.86528	-1.09335
C	-0.94799	1.52518	-1.94321	H	2.55532	5.05309	2.89363
C	-1.86836	-2.3603	2.26253	H	1.14542	6.0243	2.44001
C	2.21649	-3.50286	0.73721	H	3.12887	6.95943	-0.51438
C	2.80747	-2.53579	-0.08928	H	-3.62413	-3.05964	4.13273
C	4.17446	-2.61982	-0.37786	H	-3.60096	-1.27443	3.93462
C	4.9495	-3.65474	0.13727	H	-4.94606	-2.24002	3.22715
C	4.35129	-4.62004	0.95929	H	-0.80888	3.10518	1.782
C	3.00004	-4.53851	1.25727	H	-0.88969	4.87729	2.04699
C	1.99223	-1.40474	-0.69971	H	-0.17313	4.22311	0.53955
C	2.29643	-0.03999	-0.1392	H	-6.97635	2.17287	-0.32645
C	2.58668	0.807	-1.13993	H	6.56419	-3.06638	-0.71174
C	2.78659	2.24911	-1.14769	O	-1.22695	-2.33273	3.28185
C	2.44817	3.04325	-0.11132	O	-2.25304	0.43966	1.63664
C	2.6393	4.47959	-0.16592	O	-1.05559	2.16178	-0.91727
C	2.33498	5.38656	0.79242	O	6.27411	-3.77734	-0.12192
C	1.73843	5.13557	2.1581	O	-7.01204	1.53106	-1.05132
C	2.67534	6.78675	0.48754	O	-2.63581	-1.7742	-1.06971
C	2.60514	0.00838	-2.39495	O	2.30825	-1.27172	-2.09395
C	-3.87783	-2.22745	3.46341	O	0.96397	3.97101	2.2751
C	-0.2838	4.0564	1.62453	O	0.88453	-3.50885	1.06383
H	-4.94808	1.63639	0.69663	O	2.49604	7.71005	1.25515
H	-6.64752	-0.33041	-2.74214	O	2.83128	0.36914	-3.51846
H	-4.6995	-1.90645	-2.87328	O	-3.19395	-2.36839	2.21735

Table S14. Atomic coordinates (Å) of 1k obtained at the Cam-B3LYP/6-311+G(d,p) level of theory in the MeOH.

C	3.75077	0.98899	-1.14772	H	1.5863	3.33566	0.39521
C	3.82242	0.00537	-0.16388	H	-0.57055	1.55142	1.59319
C	4.90362	-0.8791	-0.07835	H	-0.2727	2.54693	-1.28234
C	5.91431	-0.74906	-1.02289	H	0.20638	-0.15696	0.08743
C	5.83076	0.2495	-2.02031	H	0.4198	1.59878	-3.27404
C	4.75854	1.12752	-2.10171	H	0.76695	-0.05246	-4.08314
C	2.61869	0.15028	0.64607	H	1.04795	-2.01701	-2.93541
C	1.79627	1.24793	-0.05022	H	-4.63177	1.87208	-1.02472
C	1.28353	2.38931	0.8694	H	-4.95845	5.43371	1.35939
C	-0.23344	2.28158	0.83394	H	-2.51283	5.28333	1.8965
C	-0.50729	1.74789	-0.55919	H	-2.21055	-0.18469	0.92386
C	0.50051	0.61003	-0.64705	H	-3.19469	-2.67732	-2.06841
C	0.67872	-0.07249	-1.97285	H	-2.02193	-2.60808	0.79485
C	0.6199	0.52962	-3.16836	H	-3.08591	-4.86146	-1.09326
C	0.94784	-1.52722	-1.94228	H	-2.56481	-5.05415	2.89499
C	1.87306	2.36204	2.2598	H	-1.15317	-6.02197	2.43983
C	-2.21143	3.50609	0.73571	H	-3.13842	-6.9554	-0.514
C	-2.80365	2.53923	-0.09009	H	3.63046	3.06229	4.12783
C	-4.17077	2.62422	-0.3779	H	3.60534	1.27675	3.93298
C	-4.94469	3.65986	0.13746	H	4.95111	2.23964	3.22314
C	-4.34524	4.6249	0.95891	H	0.16391	-4.21842	0.5442
C	-2.99387	4.54247	1.25604	H	0.79608	-3.09821	1.78647
C	-1.98971	1.40724	-0.70055	H	0.88095	-4.86992	2.0525
C	-2.29555	0.04292	-0.13989	H	6.96899	-2.18939	-0.32438
C	-2.58701	-0.8038	-1.14049	H	-6.56076	3.07154	-0.70895
C	-2.78866	-2.24567	-1.14821	O	1.23215	2.33716	3.27951
C	-2.45338	-3.03991	-0.1109	O	2.2521	-0.43968	1.63881
C	-2.64591	-4.47606	-0.16543	O	1.05621	-2.16303	-0.91591
C	-2.34354	-5.38332	0.79325	O	-6.26931	3.78356	-0.12108
C	-1.74762	-5.1337	2.15943	O	7.00781	-1.54669	-1.04831
C	-2.68554	-6.78309	0.48828	O	2.63964	1.76938	-1.07073
C	-2.60458	-0.00526	-2.39557	O	-2.30615	1.27449	-2.09477
C	3.88297	2.22862	3.45991	O	-0.97513	-3.96813	2.27874
C	0.27337	-4.05075	1.62915	O	-0.87923	3.5112	1.0614
H	4.94409	-1.64407	0.7002	O	-2.50822	-7.70641	1.25634
H	6.64788	0.31378	-2.74152	O	-2.83149	-0.36584	-3.51901
H	4.70383	1.89442	-2.87451	O	3.19864	2.36801	2.21391

Table S15. Atomic coordinates (Å) of 1l obtained at the Cam-B3LYP/6-311+G(d,p) level of theory in the MeOH.

C	-3.74848	-0.99574	-1.14778	H	-1.58024	-3.33833	0.39568
C	-3.82184	-0.012	-0.1642	H	0.57382	-1.5504	1.59325
C	-4.90461	0.8706	-0.07894	H	0.2777	-2.54665	-1.28218
C	-5.91514	0.73837	-1.02334	H	-0.20616	0.15656	0.08744
C	-5.82985	-0.26031	-2.02048	H	-0.41523	-1.59951	-3.27405
C	-4.756	-1.13633	-2.10174	H	-0.7658	0.051	-4.08316
C	-2.61795	-0.15471	0.64591	H	-1.05184	2.01479	-2.93543
C	-1.79358	-1.25102	-0.05016	H	4.63543	-1.86389	-1.02442
C	-1.2789	-2.39142	0.86965	H	4.96817	-5.42543	1.35908
C	0.2379	-2.2812	0.83406	H	2.52231	-5.2794	1.89608
C	0.51081	-1.74715	-0.55907	H	2.2103	0.18849	0.9241
C	-0.49893	-0.61102	-0.64701	H	3.19113	2.68296	-2.06754
C	-0.67827	0.07113	-1.97284	H	2.0149	2.61163	0.79423
C	-0.61771	-0.53079	-3.16837	H	3.07709	4.8669	-1.09264
C	-0.95077	1.52523	-1.94228	H	2.55322	5.0567	2.89516
C	-1.86829	-2.36482	2.26012	H	1.14114	6.02391	2.44001
C	2.21791	-3.50238	0.73573	H	3.12624	6.96081	-0.51281
C	2.80849	-2.53441	-0.08997	H	-3.624	-3.06811	4.12857
C	4.17575	-2.61695	-0.37773	H	-3.60252	-1.28257	3.93321
C	4.95148	-3.65126	0.13762	H	-4.94643	-2.24839	3.22382
C	4.35361	-4.61757	0.95873	H	-0.89161	4.8712	2.05015
C	3.00209	-4.53756	1.25581	H	-0.17357	4.22016	0.54211
C	1.99258	-1.40384	-0.70038	H	-0.80597	3.09953	1.78389
C	2.29572	-0.03895	-0.13965	H	-6.97353	2.1755	-0.32385
C	2.58567	0.80834	-1.14023	H	6.56674	-3.06052	-0.70886
C	2.78474	2.25058	-1.14783	O	-1.22729	-2.33882	3.27975
C	2.44679	3.04422	-0.11094	O	-2.25224	0.43635	1.63831
C	2.6371	4.48068	-0.16515	O	-1.06089	2.16077	-0.91594
C	2.33276	5.38729	0.79354	O	6.27645	-3.77247	-0.12035
C	1.73636	5.13627	2.15925	O	-7.01007	1.53405	-1.049
C	2.67294	6.78762	0.48913	O	-2.63597	-1.77412	-1.07067
C	2.60491	0.00987	-2.39532	O	2.3088	-1.27044	-2.09456
C	-3.87829	-2.23515	3.46044	O	0.96464	3.97003	2.27722
C	-0.28354	4.0523	1.62699	O	0.88577	-3.50968	1.06159
H	-4.9464	1.63573	0.69939	O	2.49357	7.71054	1.2572
H	-6.64693	-0.3263	-2.74159	O	2.83095	0.37093	-3.51877
H	-4.69987	-1.90334	-2.87434	O	-3.19385	-2.37346	2.2144

Table S16. Atomic coordinates (Å) of 1m obtained at the Cam-B3LYP/6-311+G(d,p) level of theory in the MeOH.

C	3.74785	0.99766	-1.14793	H	1.57832	3.33936	0.39531
C	3.82176	0.01411	-0.16418	H	-0.57452	1.55029	1.59333
C	4.905	-0.8679	-0.07881	H	-0.27922	2.54639	-1.28226
C	5.91532	-0.73539	-1.02338	H	0.20631	-0.15644	0.0875
C	5.82942	0.26301	-2.02076	H	0.41482	1.59991	-3.27382
C	4.75518	1.13855	-2.10204	H	0.76604	-0.05039	-4.08309
C	2.61777	0.15627	0.64588	H	1.05261	-2.01429	-2.93527
C	1.79287	1.25213	-0.05028	H	-4.63665	1.86138	-1.02418
C	1.27762	2.39233	0.86946	H	-4.97109	5.42297	1.35898
C	-0.23913	2.28121	0.83402	H	-2.52519	5.27814	1.89602
C	-0.51186	1.74686	-0.55903	H	-2.2104	-0.18961	0.92435
C	0.49854	0.61132	-0.64695	H	-3.18918	-2.68485	-2.06739
C	0.67825	-0.07072	-1.97277	H	-2.014	-2.6129	0.79481
C	0.61765	0.53125	-3.16826	H	-3.07381	-4.86877	-1.0927
C	0.95109	-1.52474	-1.94216	H	-2.55109	-5.05684	2.895
C	1.86713	2.36632	2.25988	H	-1.13863	-6.02418	2.44118
C	-2.21987	3.50125	0.73572	H	-3.12052	-6.9629	-0.51324
C	-2.80997	2.53289	-0.08987	H	3.6015	1.28469	3.93323
C	-4.17728	2.61473	-0.37761	H	4.94538	2.2502	3.22332
C	-4.9535	3.64876	0.13756	H	3.62307	3.0703	4.1279
C	-4.35615	4.61538	0.95867	H	0.89395	-4.87137	2.0502
C	-3.00459	4.53603	1.25576	H	0.17599	-4.21997	0.54226
C	-1.99349	1.4027	-0.70022	H	0.80814	-3.09963	1.78439
C	-2.29597	0.0377	-0.13942	H	6.97439	-2.17199	-0.32388
C	-2.58535	-0.80984	-1.13994	H	-6.5682	3.05721	-0.70931
C	-2.78345	-2.2522	-1.14752	O	1.2262	2.34041	3.27956
C	-2.44533	-3.04568	-0.11055	O	2.25243	-0.43477	1.63843
C	-2.63442	-4.48228	-0.16503	O	1.06083	-2.16027	-0.91577
C	-2.32944	-5.38867	0.79365	O	-6.27847	3.76932	-0.12071
C	-1.73384	-5.13681	2.15958	O	7.01062	-1.53055	-1.04904
C	-2.6678	-6.78937	0.4889	O	2.63497	1.77552	-1.07085
C	-2.60502	-0.01146	-2.39509	O	-2.30967	1.26905	-2.0944
C	3.87726	2.23707	3.46007	O	-0.96238	-3.97036	2.27733
C	0.28583	-4.05241	1.62719	O	-0.8877	3.50933	1.06147
H	4.94727	-1.63286	0.69966	O	-2.48766	-7.71224	1.25685
H	6.64634	0.32916	-2.74204	O	-2.83095	-0.37271	-3.5185
H	4.69857	1.90534	-2.87481	O	3.1927	2.37495	2.21404

Table S17. Atomic coordinates (Å) of 1n obtained at the Cam-B3LYP/6-311+G(d,p) level of theory in the MeOH.

C	3.77455	0.92109	-1.14388	H	1.65046	3.3107	0.39397
C	3.82511	-0.06427	-0.16049	H	-0.5403	1.56742	1.59078
C	4.88725	-0.9716	-0.07492	H	-0.21902	2.55095	-1.28607
C	5.90106	-0.86238	-1.01892	H	0.21024	-0.15724	0.09107
C	5.83968	0.13933	-2.01493	H	0.47112	1.58457	-3.27466
C	4.78603	1.03948	-2.09668	H	0.78199	-0.07626	-4.07883
C	2.62523	0.10649	0.65012	H	1.01223	-2.04456	-2.92362
C	1.82465	1.21883	-0.04789	H	-4.59135	1.94412	-1.02654
C	1.33042	2.37049	0.869	H	-4.86318	5.51463	1.35162
C	-0.18845	2.28982	0.83078	H	-2.41894	5.33167	1.88348
C	-0.46902	1.75781	-0.56167	H	-2.20821	-0.14675	0.91594
C	0.51911	0.60216	-0.64544	H	-3.23042	-2.6179	-2.08284
C	0.68625	-0.08877	-1.96849	H	-2.07641	-2.56954	0.78804
C	0.64568	0.51124	-3.16588	H	-3.16684	-4.80538	-1.10604
C	0.922	-1.54931	-1.93218	H	-2.69039	-5.00841	2.88895
C	1.91658	2.33401	2.26063	H	-1.28761	-5.99419	2.44555
C	-2.14524	3.5467	0.72745	H	-3.26707	-6.89708	-0.52207
C	-2.75283	2.58718	-0.09575	H	3.62063	1.21464	3.93932
C	-4.11915	2.69067	-0.38135	H	4.98868	2.14744	3.232
C	-4.8778	3.73716	0.13499	H	3.68359	2.99934	4.13239
C	-4.26235	4.69633	0.95164	H	0.07111	-4.20193	0.56424
C	-2.9116	4.59592	1.24593	H	0.70819	-3.09707	1.81754
C	-1.95635	1.44271	-0.70613	H	0.76419	-4.87114	2.07581
C	-2.28734	0.08344	-0.14774	H	6.9236	-2.32923	-0.32573
C	-2.59224	-0.75669	-1.15006	H	-6.5091	3.16408	-0.69466
C	-2.82179	-2.19433	-1.16002	O	1.27298	2.32591	3.27895
C	-2.50883	-2.99453	-0.12039	O	2.24658	-0.47591	1.64281
C	-2.72867	-4.42666	-0.17453	O	1.01461	-2.18404	-0.90369
C	-2.45432	-5.33755	0.78916	O	-6.20188	3.8781	-0.11738
C	-1.86744	-5.09757	2.16089	O	6.97683	-1.68376	-1.0462
C	-2.82195	-6.73081	0.48467	O	2.67913	1.72364	-1.06744
C	-2.59237	0.04334	-2.40427	O	-2.27172	1.31714	-2.1013
C	3.91992	2.15976	3.46593	O	-1.08022	-3.94291	2.2896
C	0.17283	-4.04099	1.6509	O	-0.81317	3.53103	1.0535
H	4.9114	-1.73829	0.70267	O	-2.6727	-7.65479	1.25787
H	6.65883	0.18725	-2.73513	O	-2.82336	-0.31179	-3.52861
H	4.74814	1.80816	-2.86876	O	3.24203	2.31224	2.21797

Table S18. Atomic coordinates (Å) of 1o obtained at the Cam-B3LYP/6-311+G(d,p) level of theory in the MeOH.

C	-3.68738	-1.16572	-1.15088	H	-1.37613	-3.43583	0.3087
C	-3.79555	-0.20763	-0.1454	H	0.65148	-1.5463	1.57216
C	-4.91748	0.62097	-0.02965	H	0.44639	-2.51833	-1.31955
C	-5.93179	0.45998	-0.9659	H	-0.20344	0.14048	0.06775
C	-5.8106	-0.5116	-1.98567	H	-0.26612	-1.60177	-3.30172
C	-4.69763	-1.33364	-2.09733	H	-0.72835	0.02328	-4.10539
C	-2.57711	-0.31147	0.64887	H	-1.17205	1.9534	-2.94881
C	-1.71062	-1.35323	-0.07912	H	4.76188	-1.56618	-0.98349
C	-1.13783	-2.48664	0.81345	H	5.27613	-5.12456	1.37242
C	0.3693	-2.28431	0.79811	H	2.82389	-5.14508	1.85825
C	0.62362	-1.71518	-0.58475	H	2.1862	0.30946	0.9281
C	-0.45085	-0.63965	-0.66997	H	3.04168	2.87849	-2.03899
C	-0.66604	0.03606	-1.99375	H	1.83698	2.71992	0.80748
C	-0.5477	-0.55155	-3.19208	H	2.78235	5.0446	-1.05698
C	-1.04737	1.46528	-1.95771	H	2.20099	5.18502	2.92343
C	-1.74068	-2.53785	2.19694	H	0.73694	6.06556	2.45645
C	2.42168	-3.37894	0.71269	H	2.69046	7.13628	-0.47123
C	2.96178	-2.3638	-0.09371	H	-3.53224	-1.59801	3.8948
C	4.33394	-2.35121	-0.35542	H	-4.83073	-2.58372	3.1298
C	5.17039	-3.33541	0.16654	H	-3.48679	-3.38976	4.01489
C	4.62403	-4.34992	0.96289	H	-1.21396	4.79426	2.02809
C	3.26266	-4.36454	1.23481	H	-0.43715	4.18169	0.53313
C	2.08403	-1.28236	-0.70747	H	-1.0196	3.02979	1.77103
C	2.29693	0.09476	-0.13603	H	-7.05438	1.82569	-0.22286
C	2.5433	0.96476	-1.12865	H	6.96445	-4.00105	0.2985
C	2.65163	2.41661	-1.12651	O	-1.11043	-2.52505	3.22351
C	2.25246	3.18253	-0.09049	O	-2.22836	0.27332	1.65108
C	2.3549	4.6282	-0.13673	O	-1.21819	2.08318	-0.92883
C	1.98313	5.51041	0.82095	O	6.49294	-3.26762	-0.12273
C	1.38854	5.21736	2.17908	O	-7.06457	1.20137	-0.96344
C	2.23716	6.93063	0.5246	O	-2.53871	-1.89249	-1.10237
C	2.62637	0.17667	-2.38772	O	2.40665	-1.1213	-2.09721
C	-3.76635	-2.53953	3.37933	O	0.6889	4.00549	2.28499
C	-0.55247	4.01134	1.61707	O	1.0873	-3.47504	1.01499
H	-4.98668	1.36625	0.76579	O	1.98951	7.83768	1.29265
H	-6.63191	-0.60078	-2.69942	O	2.84227	0.55787	-3.50645
H	-4.61406	-2.08043	-2.88703	O	-3.06441	-2.59872	2.13661

Table S19. Atomic coordinates (Å) of 1p obtained at the Cam-B3LYP/6-311+G(d,p) level of theory in the MeOH.

C	3.02786	-2.39154	-1.20944	H	3.78789	0.96676	-0.4796
C	2.7672	-2.88826	0.06524	H	1.62914	1.79267	1.49653
C	2.91893	-4.24444	0.37669	H	1.43503	1.56988	-1.54572
C	3.3346	-5.09344	-0.6419	H	0.40176	-0.18601	0.7482
C	3.58968	-4.58047	-1.93459	H	0.86898	-0.18592	-3.04778
C	3.4419	-3.23448	-2.24032	H	-0.51531	-1.43829	-3.18754
C	2.36523	-1.74367	0.87463	H	-1.60918	-2.33738	-1.42183
C	2.32446	-0.55474	-0.10004	H	-1.65805	4.56825	-0.7844
C	3.10633	0.71246	0.34642	H	1.45829	7.45785	-0.13957
C	2.06088	1.8099	0.47885	H	3.07991	5.5941	0.28983
C	1.01185	1.41136	-0.53914	H	-0.79972	1.96639	1.77503
C	0.84497	-0.07635	-0.25497	H	-3.24579	0.8466	2.08822
C	0.01035	-0.87129	-1.21999	H	-4.40464	-0.01949	-0.63725
C	0.13449	-0.82673	-2.55416	H	-5.20467	-0.48487	2.362
C	-1.04336	-1.75135	-0.6643	H	-7.51066	-2.07593	-0.76533
C	3.94642	0.50394	1.58468	H	-6.07554	-1.16518	-1.28988
C	1.62207	4.05059	-0.00876	H	-7.75609	-2.96872	1.44234
C	0.28462	3.75618	-0.31316	H	6.17159	-1.73817	2.24624
C	-0.61673	4.80108	-0.54418	H	6.19662	-0.05599	2.88613
C	-0.20077	6.12783	-0.48378	H	4.8901	-1.18401	3.38308
C	1.13833	6.4157	-0.18482	H	-4.0567	-4.10253	-1.24723
C	2.03538	5.38574	0.05307	H	-4.1344	-2.39204	-1.77668
C	-0.20597	2.31906	-0.40573	H	-3.93664	-2.79254	-0.03742
C	-1.10392	1.90845	0.72901	H	3.31844	-6.67431	0.44568
C	-2.25468	1.40926	0.2481	H	-1.9295	6.84567	-0.90488
C	-3.32644	0.77847	0.999	O	3.86928	1.163	2.59021
C	-4.33219	0.06739	0.44818	O	2.07661	-1.6635	2.04807
C	-5.28112	-0.64353	1.28017	O	-1.30125	-1.84026	0.51655
C	-6.21881	-1.51635	0.84531	O	-1.03928	7.1699	-0.70387
C	-6.43458	-1.93473	-0.5864	O	3.51468	-6.42416	-0.46931
C	-7.03831	-2.22413	1.85552	O	2.8488	-1.04885	-1.327
C	-2.19328	1.53613	-1.23733	O	-1.03337	2.14207	-1.56368
C	5.55883	-0.88884	2.56295	O	-5.82367	-3.17991	-0.86068
C	-4.42223	-3.10204	-0.98029	O	2.57822	3.09448	0.22036
H	2.71367	-4.61806	1.38225	O	-6.97113	-2.04149	3.05273
H	3.91285	-5.28482	-2.70354	O	-2.9793	1.18503	-2.07627
H	3.64299	-2.8492	-3.24003	O	4.78761	-0.50851	1.42241

Figure S17. Uncropped images of western blot

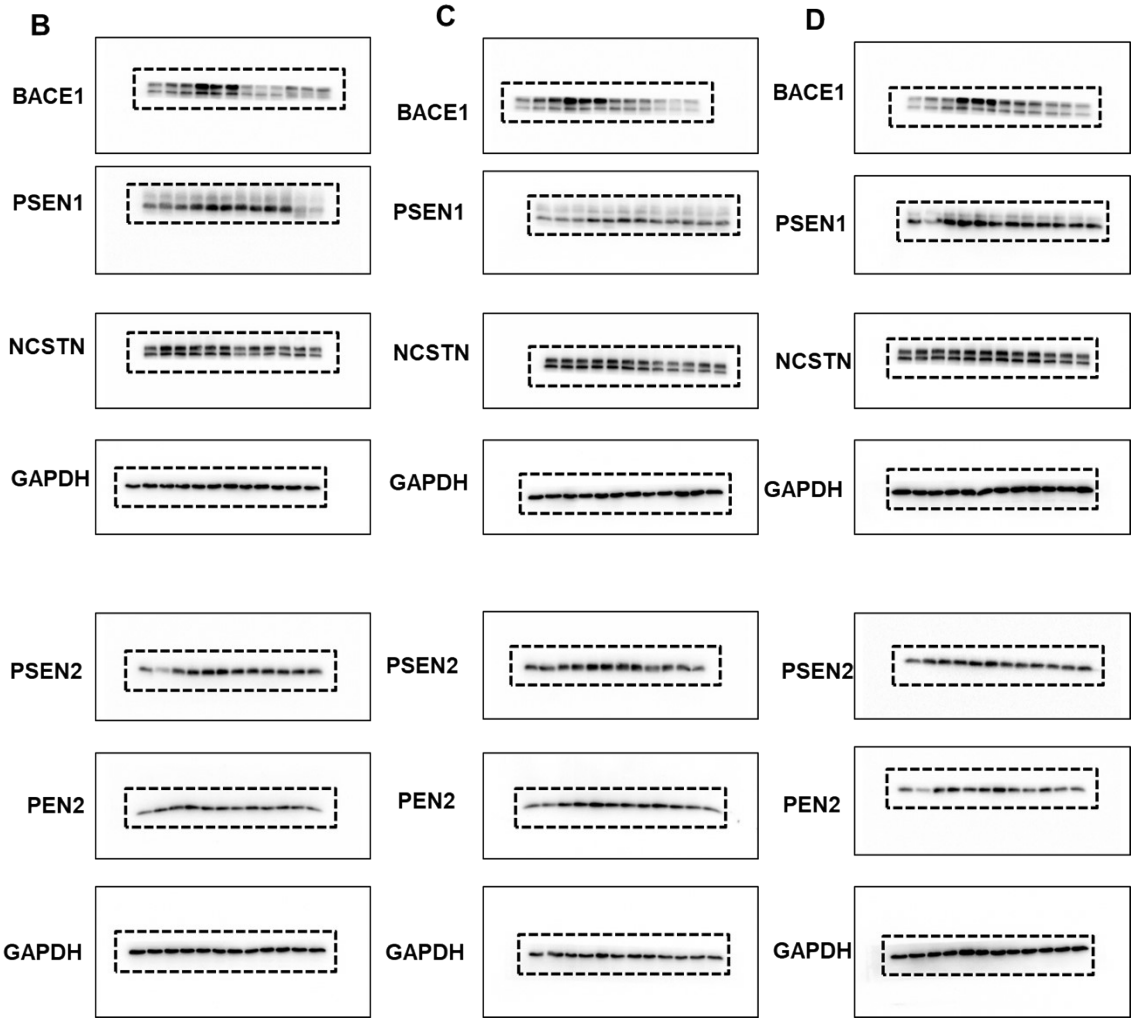

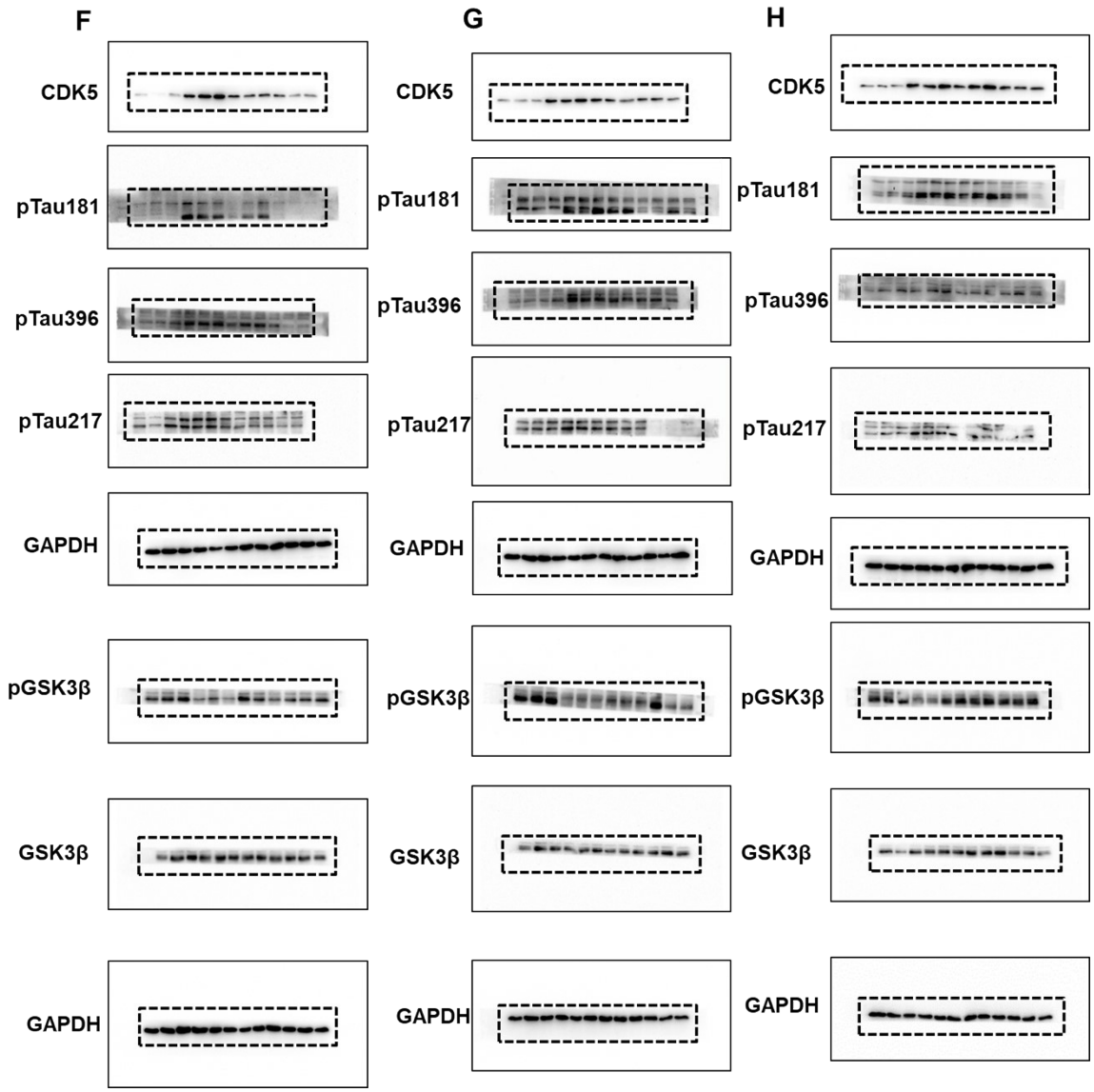

Note: B–D and F–H are corresponding to the B–D and F–H in Figure 4 of paper.

Figure S18. The molecular docking mode of (+)-1 and (–)-1 with BACE1.

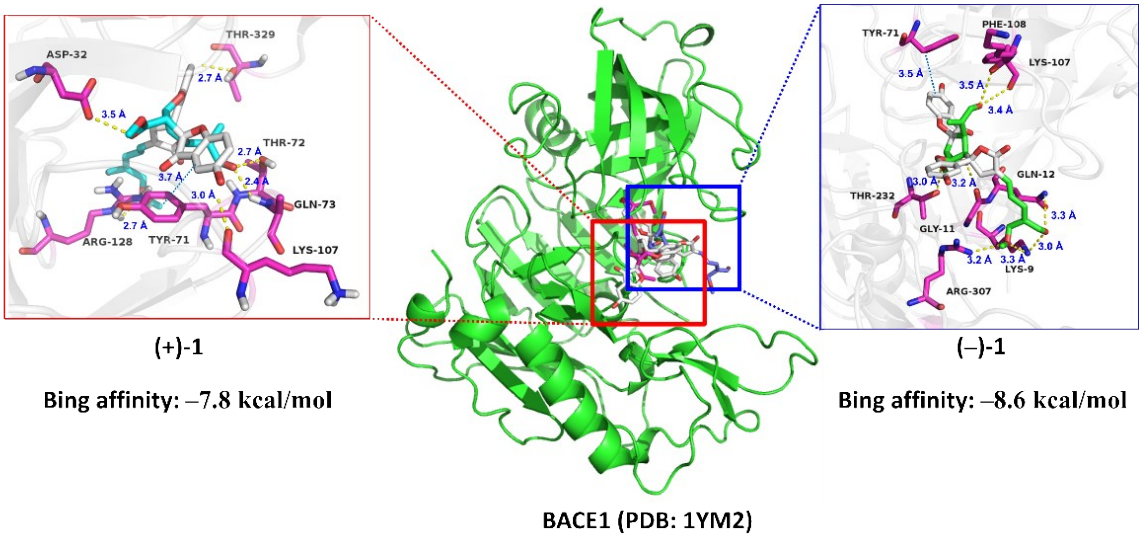

Molecular docking method: The crystal structures of BACE1 (PDB code: 1YM2)was used for preparing the new docking templates through Swiss-model server.[26] After removed the peptide and inhibitors, hydrogens were added for new models. The best confirmation was refined with energy minimization and molecular docking was performed by Autodock Vina with center box: x = 33.469, y = 0.459, z = 20.935 and the dimensions: 58 × 56 × 50 Å for BACE1. The docking results were analyzed and shown with Discovery Studio® Visualizer (BIOVIA, San Diego, USA) and PyMOL software (Schrödinger, LLC: NY, USA).

Results: The further molecular docking experiment displayed that (+)-**1** can form eight hydrogen bonds with residue PHE108, LYS107, GLN32, LYS9, ARG307, and THR232, as well as one hydrophobic bond with TYR71. Meanwhile, (–)-**1** had six hydrogen bonds with THR329, THR72, GLN73, LYS107, AGR128, and ASP32, as well as one hydrophobic bond with TYR71. Moreover, the binding energy of (–)-**1** was -8.6 kcal/mol, while that of (+)-**1** was -7.8 kcal/mol, which suggested that the binding effect of (–)-**1** was stronger than that of (+)-**1**.

Scheme S1. The proposal biosynthetic pathway for (±)-1.